Electronic Supporting Information for

"Rapid relaxation NMR measurements to predict rate coefficients in ionic liquid mixtures. An examination of reaction outcome changes in a homologous series of ionic liquids"

Daniel C. Morris,[a,b] Stuart W. Prescott[a,*] and Jason B. Harper[b,*]

[a]School of Chemical Engineering and [b]School of Chemistry, University of New South Wales, Sydney, NSW, 2052, Australia

General experimental

All chemicals used were purchased from either Sigma-Aldrich, Merck or IoLiTec and used without further purification unless otherwise stated. Unless otherwise specified, water where mentioned is Milli-Q™ water. All bromoalkanes were washed with concentrated sulfuric acid, saturated sodium bicarbonate and water before being distilled immediately prior to use. *N*-Methylimidazole and 4-methylmorpholine were distilled immediately prior to use. Benzyl bromide **1** and pyridine **2** were distilled and stored either over 3 Å molecular sieves at 4 °C (benzyl bromide **1**) or additionally over sodium hydroxide pellets at -20 °C (pyridine **2**). The terminology "*in vacuo*" refers to the use of a rotary evaporator attached to a variable vacuum pump, while "under reduced pressure" refers to the use of a Schlenk line apparatus (<1 mbar). Wherever mentioned, "under microwave conditions" refers to the use of a CEM Discover SP Microwave Synthesizer, with reaction temperature maintained by variation of the reactor power output up to a maximum of 200 W.

Kinetic analyses investigating the effect of varying proportions of ionic liquid were carried out under pseudo-first order conditions (*ca*. 0.5 ml of reaction mixture, minimum 10-fold excess of pyridine - *ca*. 0.5 mol L^{-1}, *ca*. 3 mg benzyl bromide) and followed using ^1H NMR spectroscopy at 295.35 K on either a Bruker Avance III 400 (400 MHz, ^1H), Bruker Avance III 500 (500 MHz, ^1H) or Bruker Avance III 600 (600 MHz, ^1H), using a TBI, BBO or BBFO probe. Results were shown to be consistent between spectrometers and probes. The temperature of the spectrometer was set and measured using an external thermocouple prior to each experiment.

Reactions were monitored until at least 95% of the starting material **1** was consumed. Spectra were processed using MestReNova software to measure depletion of the integral at δ *ca*. 4.6 representing the benzylic protons on the starting material **1**. Calculation of the pseudo-first order rate coefficient (k_{obs}) was done using Equation S1 below, which was subsequently converted to k_2 through Equation S2.

$$[A] = [A]_0 e^{-k_{obs}t}$$

Equation S1. The exponential equation which was used to determine observed rate coefficient; [A] = the integral of the benzyl bromide signal of interest at a given time, $[A]_0$ = the integral of the benzyl bromide signal initially, k_{obs} = the pseudo-first order rate coefficient, t = time.

$$k_2 = \frac{k_{\text{obs}}}{[\text{Pyridine } \mathbf{2}]}$$

Equation S2. The equation which was used to convert the observed pseudo-first order rate coefficient to the bimolecular form; k_2 = the bimolecular rate coefficient, k_{obs} = the pseudo-first order rate coefficient, [Pyridine **2**] = the concentration of pyridine **2** in the reaction mixture.
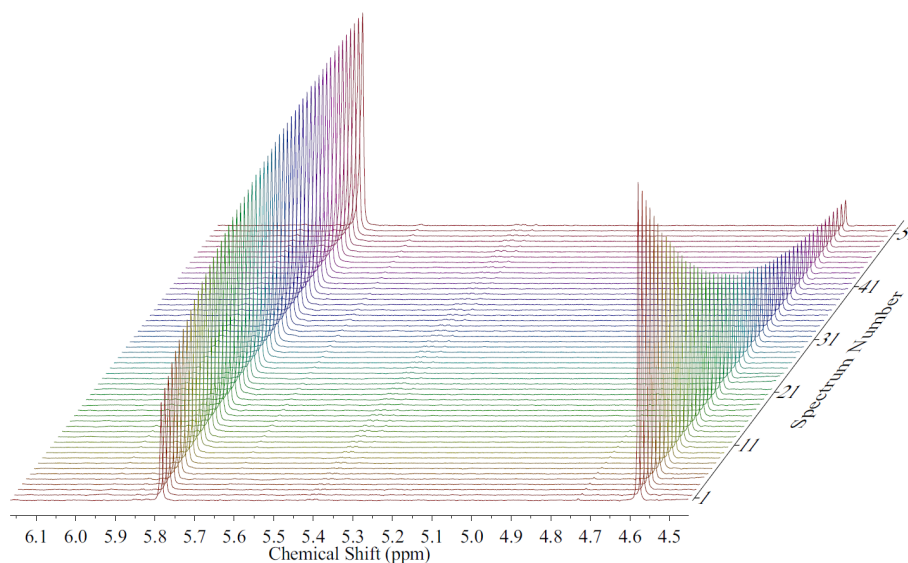
Figure S1. A representative stacked plot of NMR spectra used to calculate the bimolecular rate coefficient (k_2) associated with the reaction of benzyl bromide **1** and pyridine **2**, demonstrating the decrease in starting material **1** signal at δ *ca*. 4.6 and the increase in the signal corresponding to product **3** formation at δ *ca*. 5.8. This series of spectra were obtained following this reaction in the absence of any ionic liquid (*i.e.* in neat acetonitrile with pyridine **2** only added).

Details of the syntheses of the ionic liquids 4a–f and 5

1-Ethyl-3-methylimidazolium *bis*(trifluoromethanesulfonyl)imide ([C$_4$C$_1$im][N(SO$_2$CF$_3$)$_2$], 4a)

4a
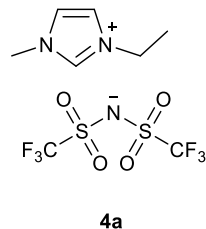
N-Methylimidazole (8.525 g, 103.8 mmol) was combined with ethyl bromide (12.99 g, 118.1 mmol) and the resulting mixture was at room temperature for two days. After this time, an opaque white solid had formed in the flask. The solid was triturated with ethyl acetate (3 x 40 ml), after which excess solvent was removed under reduced pressure. The resulting hygroscopic white powder, 1-ethyl-3-methylimidazolium bromide (19.07 g, 99.81 mmol, 96%), was used without any further purification. m.p. 72-74 °C (lit.[1] 72 °C). ^{1}H NMR (400 MHz, DMSO-d_6) δ 1.42 (t, *J* = 7.3 Hz, 3H, CH$_2$C$\underline{H}_3$), 3.85 (s, 3H, NC$\underline{H}_3$), 4.19 (q, J = 7.3 Hz, 2H, NC$\underline{H}_2$CH$_3$), 7.69 (m, 1H, NC$\underline{H}$CHN), 7.78 (m, 1H, NCHC$\underline{H}$N), 9.11 (br s, 1H, NC$\underline{H}$N).

1-Ethyl-3-methylimidazolium bromide (19.07 g, 99.81 mmol) was dissolved in water (25 ml) and the solution was combined with lithium *bis*(trifluoromethanesulfonyl)imide (31.03 g, 108.1 mmol). The resulting solution was stirred for two hours at room temperature, during which time two immiscible layers formed. The mixture was extracted using dichloromethane (3 x 30 ml), and the combined organic phases subsequently washed with water (3 x 30 ml). The organic layer was concentrated *in vacuo* and the resulting liquid was stirred under reduced pressure for 5 hours at 50 °C to give 1-ethyl-3-methylimidazolium *bis*(trifluoromethanesulfonyl)imide **4a** as a viscous, colourless liquid (38.59 g, 98.36 mmol, 98 %) ^{1}H NMR (400 MHz, DMSO-d_6) δ 1.48 (t, *J* = 7.3 Hz, 3H, CH$_2$C$\underline{H}_3$), 3.84 (s, 3H, NC$\underline{H}_3$), 4.18 (q, *J* = 7.3 Hz, 2H, NC$\underline{H}_2$CH$_3$), 7.35 (m, 1H, NC$\underline{H}$CHN), 7.40 (m, 1H, NCHC$\underline{H}$N), 8.42 (br s, 1H, NC$\underline{H}$N).

1-Butyl-3-methylimidazolium *bis*(trifluoromethanesulfonyl)imide ([C$_4$C$_1$im][N(SO$_2$CF$_3$)$_2$], 4b)

4b
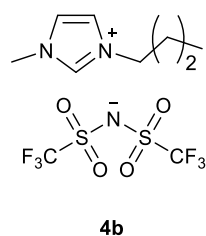
N-Methylimidazole (5.65 g, 68.8 mmol) was combined with *n*-butyl bromide (9.41 g, 68.7 mmol) and the resulting mixture was under a nitrogen atmosphere at room temperature for six days. The resulting viscous mixture was stored at 4 °C overnight. After this time, an opaque white solid had formed in the flask. The solid was triturated with ethyl acetate (3 x 40 ml), after which excess solvent was removed under reduced pressure. The resulting hygroscopic white powder, 1-butyl-3-methylimidazolium bromide (13.9 g, 62.9 mmol, 92%), was used without any further purification. ^{1}H NMR (400 MHz, Chloroform-*d*) δ 0.97 (t, *J* = 7.5 Hz, 3H, CH$_2$C$\underline{H}_3$), 1.40 (m, 2H, C$\underline{H}_2$CH$_3$), 1.91 (m, 2H,

NCH$_2$CH$_2$), 4.14 (s, 3H, NCH$_3$), 4.34 (t, J = 7.4 Hz, 2H, NCH$_2$CH$_2$), 7.44 (m, 1H, NCHCHN), 7.56 (m, 1H, NCHCHN), 10.48 (br s, 1H, NCHN).

1-Butyl-3-methylimidazolium bromide **1** (13.89 g, 62.93 mmol) was dissolved in water (75 ml) and the solution was combined with lithium *bis*(trifluoromethanesulfonyl)imide (18.82 g, 65.56 mmol). The resulting solution was stirred for two days at room temperature, during which time two immiscible layers formed. The mixture was extracted using dichloromethane (3 x 30 ml), and the combined organic phases subsequently washed with water (3 x 30 ml). The organic layer was concentrated *in vacuo* and the resulting liquid was stirred under reduced pressure for 6 hours to give 1-butyl-3-methylimidazolium *bis*(trifluoromethanesulfonyl)imide **4b** as a viscous, colourless liquid (26.14 g, 62.33 mmol, 99%) ^{1}H NMR (500 MHz, DMSO-d_6) δ 0.91 (t, J = 7.4 Hz, 3H, CH$_2$CH$_3$), 1.26 (m, 2H, CH$_2$CH$_3$), 1.77 (m, 2H, NCH$_2$CH$_2$), 3.85 (s, 3H, NCH$_3$), 4.16 (t, J = 7.2 Hz, 2H, NCH$_2$CH$_2$), 7.70 (s, 1H, NCHCHN), 7.77 (s, 1H, NCHCHN), 9.10 (br s, 1H, NCHN).

1-Hexyl-3-methylimidazolium *bis*(trifluoromethanesulfonyl)imide ([C$_6$C$_1$im][N(SO$_2$CF$_3$)$_2$], 4c)
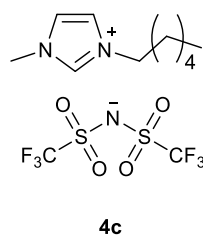
A mixture of *n*-hexyl bromide (19.9 g, 120 mmol) and *N*-methylimidazole (12.2 g, 149 mmol) was stirred at 45 °C for 2 days. Additional *n*-hexyl bromide (3.62 g, 21.9 mmol) was added to the solution and the reaction was stirred for a further 4 days. A clear viscous liquid resulted, which was then mixed thoroughly with ethyl acetate (20 mL) and the mixture was stored -19 °C overnight. Two separate liquid layers formed with no crystallisation. The ethyl acetate was removed under reduced pressure and a mixture of acetonitrile (20 mL) and ethyl acetate (20 mL) was added to the residue and the biphasic system mixed thoroughly. The mixture was stored at -19 °C overnight but again no crystallisation occurred. The acetonitrile-ethyl acetate mix was removed under reduced pressure. Acetonitrile (30 mL) was added to the residue and the resulting system was mixed before addition of ethyl acetate (10 mL). The solution was cooled using liquid nitrogen, but no crystallisation occurred. The organic solvent was decanted, diethyl ether (25 mL) was added and the resulting system was mixed thoroughly. The mixture was allowed to settle before cooling with liquid nitrogen. A viscous, opaque, white lower layer separated from the ether. The ether was decanted and the process was repeated twice more. The residue was then heated to 90 °C *in vacuo* for 6 hours to yield 1-hexyl-3-methylimidazolium bromide as a clear viscous liquid (34.4 g, 139 mmol, 98%) that was used without any further purification. ^{1}H NMR (500 MHz, Chloroform-*d*) δ 0.88 (t, J = 7.0 Hz, 3H, CH$_2$CH$_3$), 1.33 (m, 6H, CH$_2$(CH$_2$)$_3$CH$_3$), 1.92 (m, 2H, NCH$_2$CH$_2$), 4.14 (s, 3H, NCH$_3$), 4.33 (t, J = 7.5 Hz, 2H, NCH$_2$CH$_2$), 7.39 (m, 1H, NCHCHN), 7.52 (m, 1H, NCHCHN), 10.48 (s, 1H, NCHN).

1-Hexyl-3-methylimidazolium bromide (34.4 g, 13.9 mmol) was dissolved in water (20 ml) and combined with lithium *bis*(trifluoromethanesulfonyl)imide (41.1 g, 14.3 mmol) dissolved in water (25 mL). The resulting solution was stirred for three days at room temperature, during which time two immiscible layers formed. The mixture was extracted using dichloromethane (3 x 30 mL), and the combined organic phases subsequently washed with water (3 x 30 mL). The organic layer was concentrated under reduced pressure and the resulting liquid was stirred under reduced pressure for 5 hours, to give 1-hexyl-3-methylimidazolium *bis*(trifluoromethanesulfonyl)imide **4c** as a viscous, pale yellow liquid (56.5 g, 0.126 mol, 91%) that was used without any further purification. ^{1}H NMR (400 MHz, DMSO-d_6) δ 0.87 (t, J = 6.9 Hz, 3H, CH$_2$CH$_3$), 1.27 (m, 6H, CH$_2$(CH$_2$)$_3$CH$_3$), 1.78 (m, 2H, NCH$_2$CH$_2$), 3.85 (s, 3H, NCH$_3$), 4.15 (t, J = 7.5 Hz, 2H, NCH$_2$CH$_2$), 7.70 (m, 1H, NCHCHN), 7.77 (m, 1H, NCHCHN), 9.10 (s, 1H, NCHN).

1-Octyl-3-methylimidazolium *bis*(trifluoromethanesulfonyl)imide ([C$_8$C$_1$im][N(SO$_2$CF$_3$)$_2$], 4d)
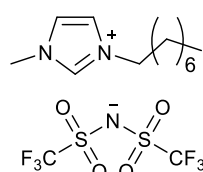
4d

N-Methylimidazole (8.94 g, 109 mmol) was combined with *n*-octyl bromide (20.5 g, 106 mmol). The resultant mixture was seen to separate into two immiscible layers. To this mixture, diethyl ether (5 mL) and acetonitrile (5 mL) were added; after this addition a single layer formed. The solution was stirred under a nitrogen atmosphere at reflux for eight days. During this time, a clear, viscous liquid formed, which was combined with ethyl acetate (40 mL) and mixed thoroughly before being allowed to settle; the result was two phases, the lower being white and opaque. The upper layer was decanted off before repeating this procedure twice more. Solvent was removed from the cloudy layer under reduced pressure before drying *in vacuo*, to yield a clear, viscous liquid. ^{1}H NMR analysis of the residue showed residual *N*-methylimidazole (*ca.* 1.7%) as indicated by the singlet at δ *ca.* 7.5. The above process was repeated three times with ether (30 mL each time). Again, the mixture was concentrated under reduced pressure and subsequently dried *in vacuo* to give a clear, viscous liquid. NMR analysis of this liquid again showed residual *N*-methylimidazole (*ca.* 1%, analysed as above). The residue was dissolved in a minimum amount of acetonitrile (*ca.* 15 mL) before addition of ethyl acetate (5 mL). The mixture was stirred vigorously, during which time hexane (40 mL) was added slowly; two phases formed. The upper layer was decanted from the mixture before the bottom layer was washed with hexane (2 x 40 mL). The resulting solution was concentrated under reduced pressure before drying at *ca*. 50 °C *in vacuo* for 5 hours to yield 1-octyl-3-methylimidazolium bromide (26.9 g, 97.7 mmol, 92%) as a clear, viscous liquid, which was used without further purification. ^{1}H NMR (400 MHz, DMSO-d_6) δ

0.87 (t, J = 6.9 Hz, 3H, CH$_2$C$\underline{H}_3$), 1.26 (m, 10H, CH$_2$(C$\underline{H}_2$)$_5$CH$_3$), 1.78 (m, 2H, NCH$_2$C$\underline{H}_2$), 3.85 (s, 3H, NC$\underline{H}_3$), 4.16 (t, J = 7.2 Hz, 2H, NC$\underline{H}_2$CH$_2$), 7.71 (m, 1H, NC$\underline{H}$CHN), 7.78 (m, 1H, NCHC$\underline{H}$N), 9.14 (s, 1H, NC$\underline{H}$N).

1-Octyl-3-methylimidazolium bromide (26.9 g, 97.7 mmol) was dissolved in water (50 ml) and subsequently combined with lithium *bis*(trifluoromethanesulfonyl)imide (29.8 g, 10.4 mmol) and the mixture was stirred vigorously for 12 hours. During this time, two cloudy, immiscible layers formed. The bottom layer was retained, and the top, aqueous layer, was extracted with dichloromethane (3 x 30 mL). The combined organic phases were then washed with water (3 x 40 mL). The organic layer was retained and concentrated under reduced pressure before being dried *in vacuo* at 60 °C to yield 1-octyl-3-methylimidazolium *bis*(trifluoromethanesulfonyl)imide (44.6 g, 93.9 mmol, 96%), as a viscous, clear liquid which was used without any further purification. ^{1}H NMR (600 MHz, DMSO-d_6) δ 0.86 (t, J = 6.9 Hz, 3H, CH$_2$C$\underline{H}_3$), 1.26 (m, 10H, CH$_2$(C$\underline{H}_2$)$_5$CH$_3$), 1.77 (m, 2H, NCH$_2$C$\underline{H}_2$), 3.85 (s, 3H, NC$\underline{H}_3$), 4.15 (t, J = 7.2 Hz, 2H, NC$\underline{H}_2$CH$_2$), 7.70 (m, 1H, NC$\underline{H}$CHN), 7.77 (m, 1H, NCHC$\underline{H}$N), 9.10 (s, 1H, NC$\underline{H}$N).

1-Decyl-3-methylimidazolium *bis*(trifluoromethanesulfonyl)imide ([C$_{10}$C$_1$im][N(SO$_2$CF$_3$)$_2$], 4e)
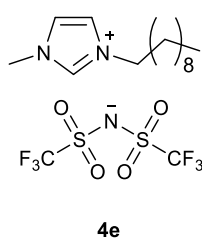

4e

N-Methylimidazole (7.59 g, 92.4 mmol) was combined with *n*-decyl bromide (20.3 g, 91.7 mmol). The resultant mixture was seen to separate into two immiscible layers. To this mixture, diethyl ether (5 mL) and acetonitrile (5 mL) were added, after this addition a single layer formed. The solution was stirred under a nitrogen atmosphere at reflux for eight days. Addition of diethyl ether (40 mL), resulted in a cloudy white solution which was stirred vigorously. The mixture was allowed to settle, the top layer was decanted off, and this process was repeated twice more. The residue was concentrated under reduced pressure to give a viscous clear liquid, and subsequently dried *in vacuo* to give a clear liquid of higher viscosity. ^{1}H NMR analysis of the residue found *N*-methylimidazole as an impurity (*ca.* 1%) by the singlet at δ *ca.* 7.5. Toluene (5 mL) and cyclohexane (25 mL) were added and the resulting system was mixed thoroughly, before the upper layer was decanted off. The residue was again washed with ether (40 mL), which was decanted off, before drying *in vacuo*. ^{1}H NMR analysis of the residue found no change in the proportion of *N*-methylimidazole, using the same analysis method as above. The crude product was dissolved in a minimum amount of acetonitrile (*ca.* 30 mL), before addition of ethyl acetate (10 mL). The mixture was stirred vigorously, during which ether (40 mL) was added slowly; two layers formed. The upper layer was decanted off, the bottom layer was then washed with hexane (3 x 40 mL). Hexane (30 mL) was added to the mixture, before allowing it to settle overnight at -19 °C. A white solid precipitated, and excess solvent was decanted. Upon equilibrating to room temperature, the solid melted. Excess hexane was decanted from the mixture and the residue was

dried *in vacuo* at *ca.* 50 °C for 5 hours to yield 1-decyl-3-methylimidazolium bromide as a highly viscous, clear liquid (27.1 g, 89.3 mmol, 97 %), which was used without any further purification. ^{1}H NMR (600 MHz, DMSO-d_6) δ 0.86 (t, *J* = 6.9 Hz, 3H, CH$_2$C$\underline{H}_3$), 1.26 (m, 14H, CH$_2$(C$\underline{H}_2$)$_7$CH$_3$), 1.78 (m, 2H, NCH$_2$C$\underline{H}_2$), 3.85 (s, 3H, NC$\underline{H}_3$), 4.15 (t, *J* = 7.2 Hz, 2H, NC$\underline{H}_2$CH$_2$), 7.71 (m, 1H, NC$\underline{H}$CHN), 7.78 (m, 1H, NCHC$\underline{H}$N), 9.14 (s, 1H, NC$\underline{H}$N).

1-Decyl-3-methylimidazolium bromide (22.7 g, 74.7 mmol) was dissolved in acetonitrile (30 mL) and water (40 mL). To this solution, lithium *bis*(trifluoromethanesulfonyl)imide was added (22.7 g, 79.0 mmol) and the mixture was stirred vigorously at room temperature for 12 hours. During this time, two clear immiscible layers formed. The bottom layer was retained, and the top, aqueous layer, was extracted with dichloromethane (3 x 30 mL). The combined organic phases were then washed with water (3 x 40 mL). The organic layer was retained and concentrated under reduced pressure before being dried *in vacuo* at 60 °C to yield 1-decyl-3-methylimidazolium *bis*(trifluoromethanesulfonyl)imide (36.8 g, 73.1 mmol, 98%), as a viscous, clear liquid which was used without any further purification. ^{1}H NMR (600 MHz, DMSO-d_6) δ 0.86 (t, *J* = 6.9 Hz, 3H, CH$_2$C$\underline{H}_3$), 1.26 (m, 14H, CH$_2$(C$\underline{H}_2$)$_7$CH$_3$), 1.77 (m, 2H, NCH$_2$C$\underline{H}_2$), 3.85 (s, 3H, NC$\underline{H}_3$), 4.15 (t, *J* = 7.2 Hz, 2H, NC$\underline{H}_2$CH$_2$), 7.70 (s, 1H, NC$\underline{H}$CHN), 7.77 (m, 1H, NCHC$\underline{H}$N), 9.10 (s, 1H, NC$\underline{H}$N).

1-Dodecyl-3-methylimidazolium *bis*(trifluoromethanesulfonyl)imide ([C$_{12}$C$_1$im][N(SO$_2$CF$_3$)$_2$], 4f)
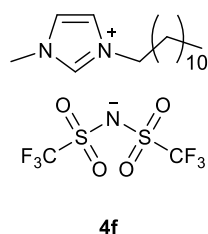

4f

N-Methylimidazole (7.51 g, 91.5 mmol) was combined with *n*-dodecyl bromide (18.9 g, 75.8 mmol). The resultant mixture was seen to separate into two immiscible layers. To this mixture, diethyl ether (5 mL) and acetonitrile (5 mL) were added, after which phase separation was still observed. Further diethyl ether (5 mL) and acetonitrile (5 mL) was added, resulting in a single phase. The solution was stirred under a nitrogen atmosphere at reflux for eight days. Diethyl ether (40 mL) was added and the mixture was shaken, resulting in precipitation. Excess solvent was decanted off, before the residue was dried *in vacuo* for 1 hour. This process was repeated twice more. The residue was found to contain *N*-methylimidazole through ^{1}H NMR analysis (*ca.* 14%, as indicated by the singlet at δ *ca.* 7.5). Acetonitrile (20 mL) was used to dissolve the residue before addition of ether (60 mL), which resulted in precipitation of a white powder. The solvent was decanted off before the residue was dried *in vacuo*. The resulting pale, yellow amorphous substance was washed with ether (2 x 40 mL), before being dried under *in vacuo* for 5 hours. During this time, an off-white solid formed, which was triturated with toluene (10 mL) and cyclohexane (40 mL). This process was repeated once more. To the white solid, a minimum amount of acetonitrile was added (*ca.* 25 ml), resulting in two distinct,

clear phases, the top presumed to be residual cyclohexane and toluene. The bottom layer was retained and combined with ether (50 ml) resulting in a white precipitate forming. Excess solvent was decanted off and the residue was dried *in vacuo* to give a white solid. ^{1}H NMR analysis of the solid showed remaining *N*-methylimidazole (*ca.* 2%, as indicated by the singlet at δ *ca.* 7.5). The white solid was crushed and combined with a mixture of ethyl acetate (5 mL) and hexane (25 mL), which was then stirred vigorously. The solvent was decanted off and the residue was washed with hexane (3 x 20 mL) to give a white solid. This solid was *in vacuo* for 5 hours, to give 1-dodecyl-3-methylimidazolium bromide as a bright, white, crystalline solid (22.9 g, 69.0 mmol, 91%) which was used without further purification. m.p. 44–46 °C (lit.[2] 43-46 °C) ^{1}H NMR (600 MHz, DMSO-d_6) δ 0.86 (t, *J* = 6.9 Hz, 3H, CH$_2$CH$_3$), 1.26 (m, 18H, CH$_2$(CH$_2$)$_9$CH$_3$), 1.77 (m, 2H, NCH$_2$CH$_2$), 3.85 (s, 3H, NCH$_3$), 4.15 (t, *J* = 7.2 Hz, 2H, NCH$_2$CH$_2$), 7.70 (m, 1H, NCHCHN), 7.77 (m, 1H, NCHCHN), 9.10 (s, 1H, NCHN).

1-Dodecyl-3-methylimidazolium bromide (22.8 g, 68.7 mmol) was dissolved in acetonitrile (30 mL) and water (40 mL). To this solution, lithium *bis*(trifluoromethanesulfonyl)imide was added (20.7 g, 72.0 mmol) and the resulting mixture was vigorously at room temperature for 12 hours. During this time, two pale yellow, immiscible layers formed. The bottom layer was retained, and the top, aqueous layer, was extracted with dichloromethane (3 x 30 mL). The combined organic phases were then then washed with water (3 x 40 mL). The organic layer was retained and concentrated under reduced pressure before being dried *in vacuo* at 60 °C to yield 1-dodecyl-3-methylimidazolium *bis*(trifluoromethanesulfonyl)imide (35.4 g, 66.6 mmol, 97%), as a viscous, pale yellow liquid which was used without any further purification. ^{1}H NMR (600 MHz, DMSO-d_6) δ 0.86 (t, *J* = 6.9 Hz, 3H, CH$_2$CH$_3$), 1.26 (m, 118H, CH$_2$(CH$_2$)$_9$CH$_3$), 1.77 (m, 2H, NCH$_2$CH$_2$), 3.85 (s, 3H, NCH$_3$), 4.15 (t, *J* = 7.2 Hz, 2H, NCH$_2$CH$_2$), 7.70 (m, 1H, NCHCHN), 7.77 (m, 1H, NCHCHN), 9.10 (s, 1H, NCHN).

4-Butyl-4-methylmorpholinium *bis*(trifluoromethanesulfonyl)imide ([C$_4$C$_1$mo][N(SO$_2$CF$_3$)$_2$], 5)
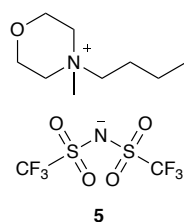
4-Methylmorpholine (1.40 g, 14 mmol) and *n*-butyl bromide (2.28 g, 17 mmol) were combined with acetonitrile (3 mL) and irradiated under microwave conditions at 100 °C for 1 hour. The acetonitrile was removed *in vacuo* to give an off-white solid. The solid was triturated with ethyl acetate (5 x 20 mL) and dried *in vacuo* to give 4-butyl-4-methylmorpholimium bromide (2.89 g, 12 mmol, 86 %) as a white solid which was used without any further purification. ^{1}H NMR (400 MHz, DMSO-d_6) δ 0.94 (t, *J* = 7.4 Hz, 3H, CH$_2$CH$_3$), 1.33 (m, 2H, CH$_3$CH$_2$), 1.67 (m, 2H, NCH$_2$CH$_2$), 3.12 (s, 3H, NCH$_3$), 3.42 (m, 6H, CH$_2$N(CH$_2$CH$_2$)$_2$O), 3.92 (m, 4H, CH$_2$N(CH$_2$CH$_2$)$_2$O).

4-Butyl-4-methylmorpholinium bromide (2.606 g, 10.95 mmol) was dissolved in water (10 ml) and the solution was combined with lithium *bis*(trifluoromethanesulfonyl)imide (3.610 g, 12.58 mmol). The resulting solution was stirred for two hours at room temperature, during which time two immiscible layers formed. The mixture was extracted using dichloromethane (2 x 25 ml), and the combined organic phases subsequently washed with water (3 x 40 ml). The organic layer was concentrated *in vacuo* and the resulting liquid was stirred under reduced pressure for 4 hours at 50 °C to give a viscous, clear liquid. This liquid was stored at 4°C for 3 hours, during which time it solidified to give 4-butyl-4-methylmorpholinium *bis*(trifluoromethanesulfonyl)imide **5** as an opaque white solid (4.405 g, 10.05 mmol, 92%), which was used without any further purification. m.p. 34-36 °C (lit.[3] 35 °C) ^{1}H NMR (400 MHz, DMSO-d_6) δ 0.95 (t, J = 7.4 Hz, 3H, CH$_2$C$\underline{H}_3$), 1.33 (m, 2H, CH$_3$C$\underline{H}_2$), 1.67 (m, 2H, NCH$_2$C$\underline{H}_2$), 3.11 (s, 3H, NCH$_3$), 3.42 (m, 6H, C$\underline{H}_2$N(C$\underline{H}_2$CH$_2$)$_2$O), 3.92 (m, 4H, CH$_2$N(CH$_2$C$\underline{H}_2$)$_2$O).

Exact composition details of mixtures used in kinetic analyses

Table S1. Composition of stock solutions by mass, including resultant mole fraction and concentration of pyridine [**2**], for the mole fraction dependent kinetic studies of the reaction between pyridine **2** and benzyl bromide **1** in mixtures of $[C_2C_1im][N(SO_2CF_3)_2]$ **4a** and acetonitrile.

Mass salt **4a** / g	Mass CH_3CN / g	Mass Pyridine **2** / g	[**2**] / mol L^{-1}	χ_{4a}
1.544	2.955	0.201	0.508	0.05
2.668	2.403	0.201	0.507	0.10
1.660	0.643	0.082	0.515	0.20
5.079	1.173	0.200	0.505	0.29
2.299	0.320	0.080	0.508	0.40
2.491	0.220	0.080	0.503	0.50
2.641	0.138	0.080	0.506	0.61
2.759	0.081	0.081	0.511	0.70
2.830	0.027	0.080	0.507	0.81

Table S2. Composition of stock solutions by mass, including resultant mole fraction and concentration of pyridine [**2**], for the mole fraction dependent kinetic studies of the reaction between pyridine **2** and benzyl bromide **1** in mixtures of $[C_6C_1im][N(SO_2CF_3)_2]$ **4c** and acetonitrile.

Mass salt **4c** / g	Mass CH_3CN / g	Mass Pyridine **2** / g	[**2**] / mol L^{-1}	χ_{4c}
1.672	2.817	0.203	0.514	0.05
2.816	2.170	0.202	0.511	0.10
4.096	1.414	0.199	0.503	0.20
4.874	0.986	0.201	0.507	0.29
5.405	0.675	0.200	0.505	0.39
2.303	0.177	0.081	0.511	0.49
2.413	0.110	0.081	0.509	0.59
6.332	0.144	0.200	0.506	0.70
2.561	0.019	0.082	0.518	0.79

Table S3. Composition of stock solutions by mass, including resultant mole fraction and concentration of pyridine [**2**], for the mole fraction dependent kinetic studies of the reaction between pyridine **2** and benzyl bromide **1** in mixtures of $[C_8C_1im][N(SO_2CF_3)_2]$ **4d** and acetonitrile.

Mass salt **4d** / g	Mass CH_3CN / g	Mass Pyridine **2** / g	[**2**] / mol L^{-1}	χ_{4d}
0.692	1.091	0.081	0.511	0.05
1.133	0.821	0.080	0.508	0.10
1.426	0.649	0.081	0.511	0.15
1.648	0.517	0.080	0.504	0.20
1.947	0.347	0.079	0.501	0.30
2.133	0.225	0.080	0.508	0.41
2.274	0.142	0.080	0.507	0.52
2.371	0.104	0.081	0.511	0.58
2.449	0.044	0.081	0.513	0.71
2.513	0.014	0.079	0.500	0.80

Table S4. Composition of stock solutions by mass, including resultant mole fraction and concentration of pyridine [**2**], for the mole fraction dependent kinetic studies of the reaction between pyridine **2** and benzyl bromide **1** in mixtures of $[C_{10}C_1im][N(SO_2CF_3)_2]$ **4e** and acetonitrile.

Mass salt **4e** / g	Mass CH_3CN / g	Mass Pyridine **2** / g	[**2**] / mol L^{-1}	χ_{4e}
2.425	0.009	0.081	0.509	0.80

Table S5. Composition of stock solutions by mass, including resultant mole fraction and concentration of pyridine [**2**], for the mole fraction dependent kinetic studies of the reaction between pyridine **2** and benzyl bromide **1** in mixtures of $[C_{12}C_1im][N(SO_2CF_3)_2]$ **4f** and acetonitrile.

Mass salt **4f** / g	Mass CH_3CN / g	Mass Pyridine **2** / g	[**2**] / mol L^{-1}	χ_{4f}
0.747	1.022	0.080	0.504	0.05
1.167	0.756	0.081	0.512	0.10
1.649	0.454	0.080	0.507	0.20
1.910	0.294	0.080	0.506	0.31
2.067	0.207	0.081	0.512	0.39
2.195	0.118	0.080	0.508	0.52
2.263	0.074	0.081	0.512	0.60
2.327	0.034	0.081	0.509	0.70
2.375	0.004	0.080	0.504	0.80

Rate coefficient data for each of the ionic liquids 4a,c-f

Table S6. The observed pseudo-first order rate coefficient (k_{obs}) and resultant bimolecular rate coefficient (k_2) associated with the reaction of benzyl bromide **1** and pyridine **2** at 22.2°C in mixtures containing different proportions of each of the ionic liquids $[C_{2n+2}C_1im][N(SO_2CF_3)_2]$ **4a,c-f** in acetonitrile, as well as the concentration of pyridine **2** used in calculation.

Ionic Liquid	χ_{IL}	[**2**] / mol L^{-1}	k_{obs}	k_2
4a	0.05	0.508	5.16	10.2
			5.25	10.3
			5.16	10.2
	0.10	0.507	5.87	11.6
			6.04	11.9
			6.19	12.2
	0.20	0.515	7.34	14.2
			6.97	13.5
			7.20	14.0
	0.29	0.505	7.95	15.7
			7.62	15.1
			7.62	15.1
	0.40	0.508	8.36	16.4
			8.48	16.7
			8.32	16.4
	0.50	0.503	8.93	17.8
			8.15	16.2
			8.54	17.0
	0.61	0.506	8.88	17.6
			8.63	17.2
			8.75	17.3
	0.70	0.511	9.30	18.2
			9.02	17.6
			8.93	17.5

	0.81	0.507	8.95	17.7
			9.87	19.5
			8.98	17.7
			8.60	17.0
4c	0.05	0.514	4.85	9.45
			4.84	9.43
			4.83	9.41
	0.10	0.511	5.31	10.4
			5.55	10.9
			5.12	10.0
	0.20	0.503	5.89	11.7
			5.84	11.6
			5.78	11.5
	0.29	0.507	5.65	11.1
			5.94	11.7
			5.87	11.6
	0.39	0.505	6.26	12.4
			6.18	12.2
			6.28	12.5
	0.49	0.511	6.17	12.1
			5.93	11.6
			5.86	11.5
	0.59	0.509	6.14	12.1
			6.23	12.3
			6.02	11.8
	0.70	0.506	6.81	13.4
			6.87	13.6
			6.77	13.4
	0.79	0.518	6.45	12.4
			6.68	12.9

			6.68	12.9
4d	0.05	0.511	3.91	7.66
			4.27	8.36
			4.08	8.00
	0.10	0.508	4.89	9.63
			5.11	10.1
			4.84	9.54
	0.15	0.511	4.98	9.75
			5.34	10.5
			5.26	10.3
	0.20	0.504	5.22	10.4
			5.23	10.4
			5.12	10.1
	0.30	0.501	5.13	10.2
			5.19	10.4
			5.22	10.4
	0.41	0.508	5.19	10.2
			5.34	10.5
			5.12	10.1
	0.52	0.507	5.23	10.3
			5.17	10.2
			5.29	10.4
	0.58	0.511	5.40	10.6
			5.13	10.0
			5.07	9.91
	0.71	0.513	5.25	10.2
			5.43	10.6
			5.03	9.82
	0.80	0.500	5.46	10.9
			5.56	11.1

			5.16	10.3
4f	0.05	0.504	3.94	7.80
			3.90	7.73
			3.94	7.82
	0.10	0.512	4.10	8.01
			4.05	7.91
			4.04	7.89
	0.20	0.507	4.40	8.68
			4.43	8.74
			4.35	8.58
	0.31	0.506	4.15	8.20
			4.36	8.62
			4.35	8.59
	0.39	0.512	4.44	8.67
			4.35	8.49
			4.33	8.45
	0.52	0.508	4.41	8.69
			4.09	8.07
			4.06	8.01
	0.60	0.512	4.14	8.08
			4.21	8.22
			4.12	8.04
	0.70	0.509	4.51	8.90
			4.28	8.45
			4.12	8.13
	0.80	0.504	3.88	7.70
			4.37	8.68
			3.98	7.91
			4.48	8.90

Exact compositions and rate coefficient data for temperature dependence analyses at χ_{IL} ca. 0.8

Table S7. Composition of stock solutions by mass, including resultant mole fraction and concentration of pyridine **2**, for the temperature dependent kinetic studies of the reaction between pyridine **2** and benzyl bromide **1** in mixtures of salts **4a,c-f** in acetonitrile.

Ionic Liquid	Mass IL / g	Mass CH$_3$CN / g	Mass Pyridine **2** / g	[**2**] / mol L^{-1}	χ_{IL}
4a	7.088	0.083	0.205	0.519	0.80
4c	6.409	0.049	0.202	0.510	0.79
4d	6.283	0.040	0.201	0.507	0.79
4f	5.937	0.009	0.202	0.509	0.80

Table S8. The observed pseudo-first order rate coefficient (k_{obs}) and resultant bimolecular rate coefficient (k_2) associated with the reaction of benzyl bromide **1** and pyridine **2** in mixtures of [C$_{2n+2}$C$_1$im][N(SO$_2$CF$_3$)$_2$] **4** in acetonitrile (χ_{IL} *ca*. 0.8) at various temperatures, as well as the concentration of pyridine **2**.

Ionic Liquid	χ_{IL}	[**2**] / mol L^{-1}	Temperature / K	k_{obs} / 10^{-4} s^{-1}	k_2 / 10^{-4} L mol^{-1} s^{-1}
4a	0.81	0.507	295.35	8.95	17.5
				9.87	17.7
				8.98	19.5
				8.60	17.7
	0.80	0.519	286.35	4.64	8.94
				4.80	9.26
				4.62	8.90
	0.80	0.519	304.95	19.8	38.1
				18.9	36.4
				20.2	38.9
	0.80	0.519	314.75	37.3	71.9
				36.5	70.3
				37.5	72.3

4c	0.79	0.518	295.35	6.45	12.4
				6.68	12.9
				6.68	12.9
	0.79	0.510	304.25	11.9	23.3
				12.1	23.8
				12.2	24.0
	0.79	0.510	313.75	23.6	46.3
				23.1	45.3
				24.1	47.2
	0.79	0.510	323.65	44.0	86.3
				46.3	90.7
				45.6	89.3
4d	0.80	0.500	295.35	5.46	10.9
				5.56	11.1
				5.16	10.3
	0.79	0.507	304.25	10.2	20.1
				10.8	21.4
				10.7	21.1
	0.79	0.507	314.15	22.4	44.2
				22.6	44.6
				21.8	43.0
	0.79	0.507	323.65	45.2	89.2
				43.4	85.6
				44.5	87.9
4f	0.80	0.504	295.35	3.88	7.70
				4.37	8.68
				3.98	7.91
				4.48	8.90
	0.80	0.509	307.45	10.7	21.0
				9.92	19.5

			10.9	21.3
0.80	0.509	316.55	19.9	39.1
			19.9	39.0
			22.3	43.8
0.80	0.509	326.65	42.1	82.7
			42.5	83.5
			44.1	86.5

Eyring plots used to determine activation parameters
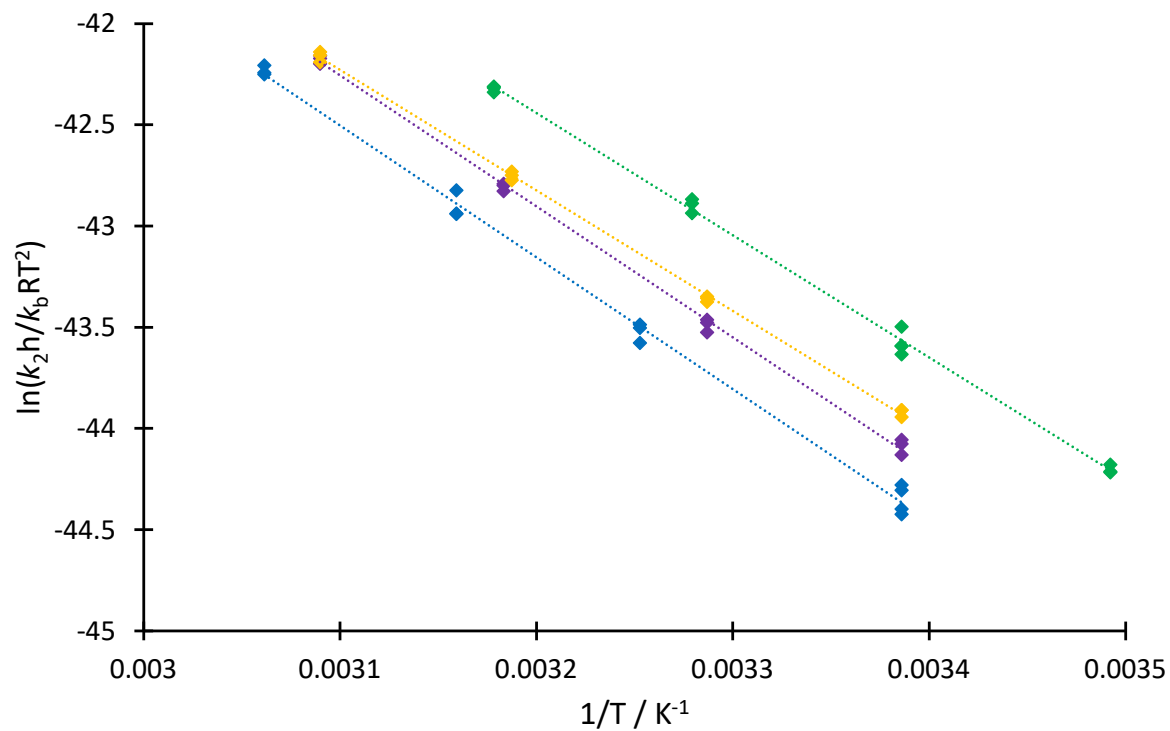
Figure S2. The Eyring plots used to determine activation parameters associated with the reaction of benzyl bromide **1** and pyridine **2** in mixtures of salts **4a** (♦), **4c** (♦), **4d** (♦) or **4f** (♦) in acetonitrile (χ_{IL} *ca.* 0.8).

Procedure for multi-component exponential fitting of relaxation data

The direct output of spin-spin relaxation measurements was processed *via* a Jupyter notebook using the Python-based 'SciPy' library of modules.[4] Full code is available upon request. Each data set was used to calculate the closest fit to Equation S3 below using a Levenberg–Marquardt non-linear least squares regression with scipy.optimize.curve_fit.

$$\frac{I(t)}{I(0)} = \phi_{\text{IL}} \times e^{\left(\frac{-t}{T_{2(\text{IL})}}\right)} + \phi_{\text{non}-\text{IL}} \times e^{\left(\frac{-t}{T_{2(\text{non}-\text{IL})}}\right)} + C$$

Equation S3. The Equation used to fit a two component exponential to the direct relaxation output; $I(t)/I(0)$ = measured ^{1}H signal intensity as a function of time (normalised to the value from the first echo), t = time, while $T_{2(\text{IL})}$ and $T_{2(\text{non-IL})}$ = spin-spin relaxation times corresponding to the 'ionic liquid component' or the remaining signals in the mixture respectively, ϕ_{IL} and $\phi_{\text{non}-\text{IL}}$ = calculated molar weighting of 'ionic liquid ^{1}H signals' or remaining ^{1}H signals, respectively ($\phi_{\text{non}-\text{IL}} = 1 - \phi_{\text{IL}}$), C = constant baseline offset representing combined zero offset of the analogue and digital parts of the received chain in the measurement (typically much less than 10% of the observed signal). The ratio of signal to rms noise is in excess of 1000:1 as can be seen in Figure S3.

ϕ_{IL} is calculated for each unique mixture composition (*cf*. Tables S9-S13). Given this fixed ϕ_{IL} (and hence by definition, fixed $\phi_{\text{non}-\text{IL}}$), the fitting algorithm only has three free parameters to return: $T_{2(\text{IL})}$, $T_{2(\text{non-IL})}$, and the associated noise component. Comparison of single exponential fits, along with residual analysis, is given in Figure S3 and demonstrates the need to use Equation S3 in these analyses.

The effectiveness of this methodology and the rationale for using the biexponential is also shown by considering the reduced χ^2 statistic for each fit (Figure S4). The reduction in this value on going from a single exponential fit to a biexponential fit is perhaps unsurprising, given the data presented above; increasing the number of exponentials further has no significant effect on the reduced χ^2 and so such analysis is not warranted.
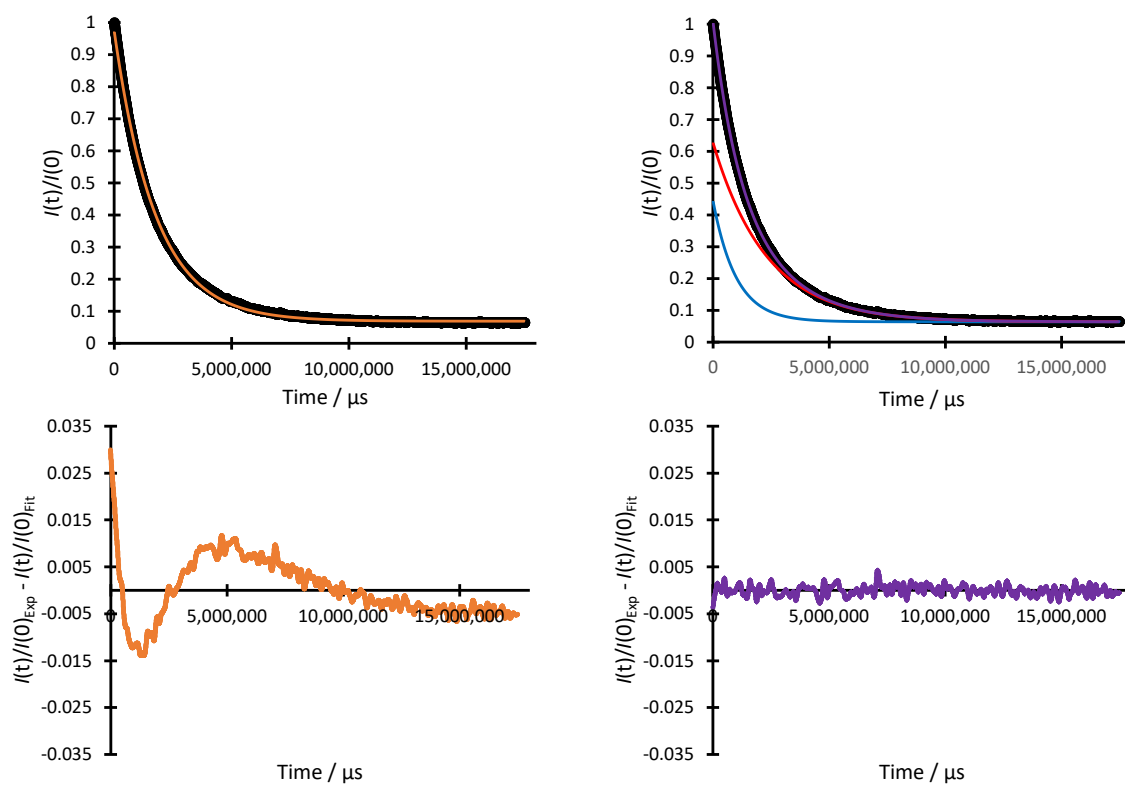
Figure S3. Representative plots (for χ_{IL} *ca*. 0.1, ionic liquid **4d**) of raw data (black), $I(t)/I(0)$, and fitted curves (left) a single exponential fit (orange) produced (right) two component fit (purple) comprised of $T_{2(IL)}$ (blue) and $T_{2(non-IL)}$ (red) along with the associated residual analysis.
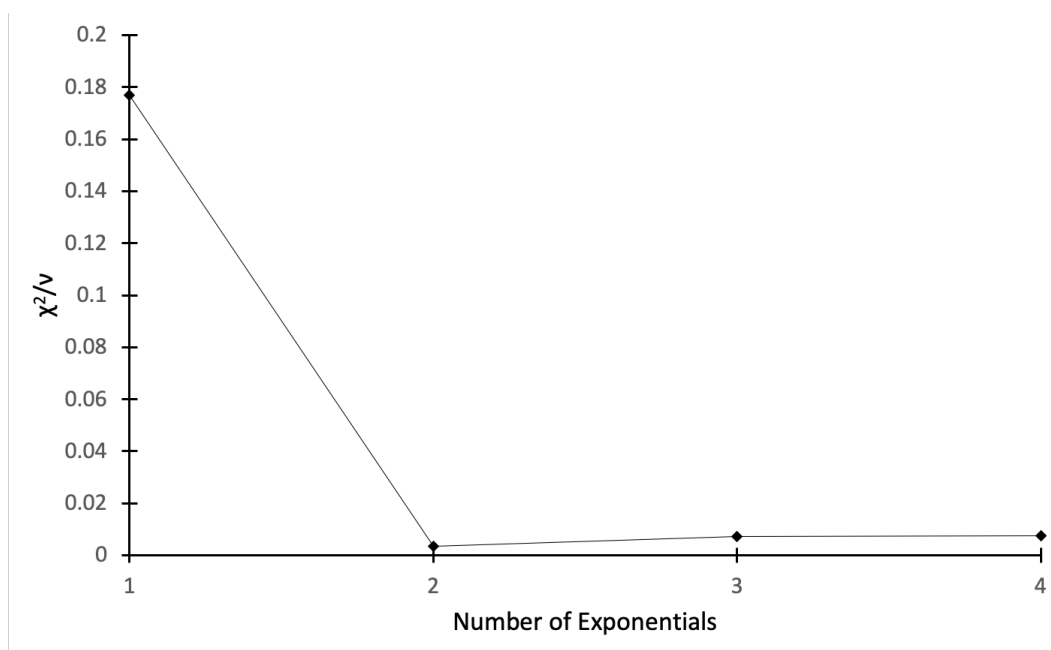

Figure S4. Reduced χ^2 for fits of $I(t)/I(0)$ (for χ_{IL} *ca*. 0.1, ionic liquid **4d**) to either 1, 2 3 or 4 exponentials.

It is important to note, that in the case of the imidazolium-based ionic liquids **4** investigated here, the aromatic protons were excluded from the 'ionic liquid component' when calculating ϕ_{IL}, as they tend to display relaxation times on a timescale not similar enough to the alkyl signals to allow accurate determination; rapid rate of exchange of these protons (particularly that in the C2 position of the $[C_{2n+2}C_1\text{im}]^+$ cation) also causes the observed signal to represent a weighted average of the relaxation time associated with the ^{1}H environments which are exchanging, complicating reliable interpretation. With this in mind, to confirm the validity of the processed $T_{2(\text{IL})}$ values, control studies were completed on representative solvent compositions involving deuteration of the acetonitrile and, in some cases, the ionic liquid. These experiments included using a sample of the butyl system **4b** that had been partially deuterated on the aromatic ring of the cation[5] and systems involving the ionic liquids **4a** and **5** in acetonitrile; in each case these data contained only a single source of protons, allowing a single exponential fit. From each of these control experiments, it was concluded that the "ionic liquid" and "non-ionic liquid" relaxation times calculated from the fitting algorithm were correctly assigned (and of the same value, validating the fitting method). Representative data are included below for comparison.

Table S9. Representative comparisons of $T_{2(\text{IL})}$ data from mixtures containing either protiated or deuterated acetonitrile and an ionic liquid at the proportion specified; in all cases the data was the same irrespective of the isotopic composition of the acetonitrile used, supporting both the assignment of relaxation times to each component of the mixture and the process through which the relaxation times were calculated.

Ionic liquid	χ_{IL}	$T_{2(\text{IL})}$ protiated case / s	$T_{2(\text{IL})}$ deuterated case[a] / s
4a	0.05	2.288 ± 0.231	2.337 ± 0.016
Partially deuterated **4b**	0.1	1.490 ± 0.048	1.491 ± 0.011
Partially deuterated **4b**	0.7	0.291 ± 0.012	0.315 ± 0.013
Partially deuterated **4b**	1	0.210 ± 0.003[b]	0.192 ± 0.002
5	0.04	1.256 ± 0.010	1.238 ± 0.008

[a]This fit is to a single exponential ('unsplit') given that there is only one source of protons.
[b]This comparison is to the parent protiated ionic liquid **4b**.

Exact compositions and associated fitting parameters for mixtures of salts 4 used in relaxation analyses

Table S10. Composition of stock solutions by mass, including resultant mole fraction, concentration of pyridine **2** and associated splitting parameter, ϕ_{IL}, for the mole fraction dependent relaxation studies for mixtures of [C$_2$C$_1$im][N(SO$_2$CF$_3$)$_2$] **4a** and acetonitrile.

Mass salt **4a** / g	Mass CH$_3$CN / g	Mass **2** / g	[**2**] / mol L^{-1}	$\chi_{\mathbf{4a}}$	ϕ_{IL}
1.544	2.955	0.201	0.508	0.05	0.1161
0.534	0.469	0.042	0.531	0.10	0.2103
1.660	0.643	0.082	0.515	0.20	0.3436
5.079	1.173	0.200	0.505	0.29	0.4307
2.299	0.320	0.080	0.508	0.40	0.5049
2.491	0.220	0.080	0.503	0.50	0.5589
2.641	0.138	0.080	0.506	0.61	0.6040
2.759	0.081	0.081	0.511	0.70	0.6367
2.830	0.027	0.080	0.507	0.81	0.6679

Table S11. Composition of stock solutions by mass, including resultant mole fraction, concentration of pyridine **2** and associated splitting parameter ϕ_{IL}, for the mole fraction dependent relaxation studies for mixtures of [C$_4$C$_1$im][N(SO$_2$CF$_3$)$_2$] **4b** and acetonitrile.

Mass salt **4b** / g	Mass CH$_3$CN / g	Mass **2** / g	[**2**] / mol L^{-1}	$\chi_{\mathbf{4b}}$	ϕ_{IL}
0.338	0.564	0.042	0.530	0.05	0.1729
0.551	0.456	0.038	0.485	0.10	0.2841
0.751	0.371	0.041	0.522	0.16	0.3794
0.842	0.298	0.041	0.521	0.21	0.4423
0.998	0.209	0.042	0.528	0.30	0.5329
1.133	0.138	0.042	0.534	0.41	0.6085
1.217	0.094	0.040	0.511	0.51	0.6578
1.275	0.061	0.043	0.541	0.60	0.6911
1.324	0.034	0.042	0.532	0.70	0.7214
1.359	0.014	0.041	0.513	0.79	0.7450

Table S12. Composition of stock solutions by mass, including resultant mole fraction, concentration of pyridine **2** and associated splitting parameter ϕ_{IL}, for the mole fraction dependent relaxation studies for mixtures of [C$_6$C$_1$im][N(SO$_2$CF$_3$)$_2$] **4c** and acetonitrile.

Mass salt **4c** / g	Mass CH$_3$CN / g	Mass **2** / g	[**2**] / mol L^{-1}	χ_{4c}	ϕ_{IL}
0.336	0.563	0.041	0.515	0.05	0.2073
2.816	2.170	0.202	0.511	0.10	0.3462
4.096	1.414	0.199	0.503	0.20	0.5054
4.874	0.986	0.201	0.507	0.29	0.5975
5.405	0.675	0.200	0.505	0.39	0.6631
2.303	0.177	0.081	0.511	0.49	0.7108
2.413	0.110	0.081	0.509	0.59	0.7466
6.332	0.144	0.200	0.506	0.70	0.7753
1.286	0.001	0.040	0.508	0.79	0.7947

Table S13. Composition of stock solutions by mass, including resultant mole fraction, concentration of pyridine **2** and associated splitting parameter ϕ_{IL}, for the mole fraction dependent relaxation studies for mixtures of [C$_8$C$_1$im][N(SO$_2$CF$_3$)$_2$] **4d** and acetonitrile.

Mass salt **4d** / g	Mass CH$_3$CN / g	Mass **2** / g	[**2**] / mol L^{-1}	χ_{4d}	ϕ_{IL}
0.692	1.091	0.081	0.511	0.05	0.2460
1.133	0.821	0.080	0.508	0.10	0.3975
1.426	0.649	0.081	0.511	0.15	0.4937
1.648	0.517	0.080	0.504	0.20	0.5656
1.947	0.347	0.079	0.501	0.30	0.6574
2.133	0.225	0.080	0.508	0.41	0.7196
2.274	0.142	0.080	0.507	0.52	0.7623
2.371	0.104	0.081	0.511	0.58	0.7828
2.449	0.044	0.081	0.513	0.71	0.8124
2.513	0.014	0.079	0.500	0.80	0.8285

Table S14. Composition of stock solutions by mass, including resultant mole fraction, concentration of pyridine **2** and associated splitting parameter ϕ_{IL}, for the mole fraction dependent relaxation studies for mixtures of $[C_{10}C_{1}im][N(SO_2CF_3)_2]$ **4e** and acetonitrile.

Mass salt **4e** / g	Mass CH$_3$CN / g	Mass **2** / g	[**2**] / mol L^{-1}	χ_{4e}	ϕ_{IL}
2.425	0.009	0.081	0.509	0.80	0.8514

Table S15. Composition of stock solutions by mass, including resultant mole fraction, concentration of pyridine **2** and associated splitting parameter ϕ_{IL}, for the mole fraction dependent relaxation studies for mixtures of $[C_{12}C_{1}im][N(SO_2CF_3)_2]$ **4f** and acetonitrile.

Mass salt **4f** / g	Mass CH$_3$CN / g	Mass **2** / g	[**2**] / mol L^{-1}	χ_{4f}	ϕ_{IL}
0.747	1.022	0.080	0.504	0.05	0.3193
1.167	0.756	0.081	0.512	0.10	0.4786
1.649	0.454	0.080	0.507	0.20	0.6463
1.910	0.294	0.080	0.506	0.31	0.7294
2.067	0.207	0.081	0.512	0.39	0.7735
2.195	0.118	0.080	0.508	0.52	0.8161
2.263	0.074	0.081	0.512	0.60	0.8365
2.327	0.034	0.081	0.509	0.70	0.8557
2.375	0.004	0.080	0.504	0.80	0.8696

Mole fraction dependent relaxation data for salts 4

Table S16. The calculated single-component (T_2) and two-component ($T_{2(IL)}$ and $T_{2(non\text{-}IL)}$) exponential decay constants, as well as the noise fraction of signal, determined in the relaxation studies of mixtures of $[C_{2n+2}C_1im][N(SO_2CF_3)_2]$ **4**, pyridine **2** and acetonitrile.

Ionic Liquid	χ_{IL}	T_2 / s	$T_{2(IL)}$ /s	$T_{2(non\text{-}IL)}$	Noise
4a	0.05	2.807	2.397	2.862	0.070
		2.817	2.003	2.937	0.071
		2.837	2.597	2.869	0.072
		2.828	2.025	2.943	0.070
		2.837	2.338	2.913	0.070
		2.739	2.371	2.788	0.069
	0.10	2.433	1.996	2.556	0.071
		2.471	1.947	2.622	0.071
		2.424	1.812	2.602	0.073
		2.433	1.819	2.612	0.072
		2.433	1.915	2.581	0.066
	0.20	1.829	1.432	2.068	0.074
		1.814	1.490	2.012	0.074
		1.803	1.461	2.005	0.075
		1.813	1.459	2.033	0.075
	0.29	1.438	1.236	1.615	0.078
		1.435	1.109	1.730	0.078
		1.440	1.181	1.675	0.078
		1.426	1.149	1.669	0.076
		1.441	1.185	1.664	0.078
	0.40	1.090	0.876	1.355	0.078
		1.096	0.926	1.296	0.079
		1.095	0.865	1.383	0.077
		1.093	0.878	1.370	0.080
		1.109	0.938	1.309	0.079

	0.50	0.890	0.752	1.108	0.080
		0.894	0.784	1.053	0.080
		0.885	0.718	1.159	0.079
		0.880	0.736	1.100	0.078
		0.892	0.768	1.084	0.081
	0.61	0.690	0.570	0.923	0.079
		0.690	0.584	0.887	0.081
		0.692	0.571	0.927	0.080
		0.699	0.603	0.872	0.083
		0.698	0.588	0.905	0.081
	0.70	0.583	0.509	0.739	0.080
		0.590	0.506	0.769	0.082
		0.587	0.502	0.778	0.081
		0.586	0.500	0.772	0.080
		0.590	0.497	0.796	0.081
	0.81	0.558	0.475	0.772	0.083
		0.549	0.490	0.694	0.086
		0.513	0.453	0.653	0.083
		0.520	0.463	0.656	0.084
		0.526	0.473	0.649	0.084
		0.526	0.479	0.639	0.085
4b	0.05	2.610	1.677	2.835	0.067
		2.607	1.682	2.829	0.067
		2.620	1.663	2.852	0.068
	0.10	2.175	1.484	2.522	0.067
		2.133	1.468	2.442	0.070
		2.211	1.534	2.534	0.071
		2.159	1.452	2.493	0.067
		2.126	1.441	2.450	0.067
		2.173	1.561	2.474	0.069

0.16	1.714	1.108	2.192	0.073
	1.696	1.103	2.162	0.075
	1.687	1.171	2.099	0.067
	1.717	1.121	2.201	0.073
0.20	1.421	0.996	1.859	0.074
	1.399	1.005	1.814	0.070
	1.425	1.002	1.863	0.071
	1.480	1.059	1.922	0.075
0.30	1.015	0.758	1.397	0.078
	1.028	0.762	1.441	0.074
	1.014	0.752	1.423	0.072
	1.057	0.810	1.438	0.077
0.41	0.697	0.519	1.093	0.074
	0.706	0.534	1.101	0.076
	0.696	0.539	1.036	0.074
	0.738	0.588	1.063	0.078
0.51	0.528	0.425	0.800	0.079
	0.530	0.433	0.789	0.078
	0.515	0.417	0.776	0.074
	0.554	0.441	0.886	0.074
0.60	0.437	0.359	0.680	0.075
	0.431	0.348	0.707	0.074
	0.423	0.356	0.620	0.075
	0.457	0.387	0.682	0.077
0.70	0.335	0.283	0.520	0.071
	0.335	0.290	0.500	0.078
	0.327	0.281	0.484	0.072
	0.349	0.309	0.480	0.079
0.79	0.275	0.239	0.426	0.074
	0.278	0.242	0.422	0.075

		0.267	0.229	0.422	0.073
		0.271	0.233	0.426	0.073
		0.270	0.234	0.415	0.070
		0.273	0.243	0.379	0.073
		0.272	0.236	0.417	0.068
		0.286	0.244	0.479	0.069
4c	0.05	2.325	1.195	2.672	0.066
		2.314	1.224	2.655	0.066
		2.375	1.218	2.730	0.067
		2.381	1.254	2.731	0.066
		2.378	1.264	2.724	0.065
		2.382	1.168	2.759	0.061
		2.381	1.231	2.739	0.059
		2.370	1.263	2.713	0.057
	0.10	1.695	0.976	2.193	0.069
		1.696	0.973	2.198	0.068
		1.694	0.984	2.184	0.068
		1.704	0.981	2.207	0.068
		1.680	0.961	2.219	0.067
	0.20	1.068	0.696	1.618	0.069
		1.064	0.684	1.644	0.066
		1.067	0.694	1.634	0.067
		1.068	0.690	1.644	0.068
		1.064	0.688	1.639	0.068
	0.29	0.711	0.515	1.166	0.070
		0.715	0.516	1.173	0.071
		0.718	0.512	1.207	0.068
		0.722	0.520	1.191	0.070
	0.39	0.460	0.345	0.842	0.067
		0.462	0.356	0.801	0.071

	0.460	0.350	0.813	0.071
	0.462	0.353	0.812	0.071
	0.465	0.350	0.845	0.068
0.49	0.356	0.280	0.676	0.066
	0.357	0.278	0.720	0.064
	0.357	0.279	0.712	0.063
	0.357	0.279	0.707	0.065
	0.358	0.278	0.726	0.068
	0.358	0.277	0.736	0.061
	0.356	0.277	0.719	0.067
	0.358	0.278	0.726	0.064
0.60	0.258	0.212	0.491	0.070
	0.257	0.207	0.530	0.061
	0.257	0.211	0.486	0.067
	0.256	0.208	0.509	0.065
	0.257	0.210	0.506	0.063
	0.258	0.211	0.496	0.064
	0.258	0.212	0.487	0.065
0.70	0.196	0.167	0.366	0.067
	0.198	0.166	0.391	0.064
	0.200	0.167	0.416	0.060
	0.199	0.168	0.385	0.066
0.79	0.163	0.136	0.385	0.050
	0.164	0.137	0.384	0.050
	0.161	0.135	0.370	0.054
	0.162	0.137	0.336	0.059
	0.163	0.137	0.355	0.056
	0.164	0.137	0.372	0.052
	0.164	0.139	0.343	0.060

4d	0.05	2.301	1.173	2.755	0.069
		2.291	1.204	2.727	0.067
		2.207	1.125	2.634	0.066
		2.296	1.171	2.760	0.067
		2.326	1.195	2.785	0.067
	0.10	1.610	0.936	2.254	0.068
		1.603	0.936	2.237	0.066
		1.562	0.934	2.146	0.067
		1.606	0.938	2.258	0.068
		1.628	0.977	2.232	0.068
		1.613	0.954	2.238	0.068
	0.15	1.213	0.747	1.912	0.070
		1.210	0.769	1.851	0.073
		1.185	0.724	1.861	0.064
		1.216	0.767	1.917	0.068
		1.224	0.779	1.912	0.069
		1.226	0.788	1.896	0.070
		1.193	0.723	1.882	0.066
	0.20	0.904	0.598	1.531	0.070
		0.914	0.619	1.575	0.070
		0.922	0.635	1.553	0.071
		0.926	0.623	1.563	0.071
	0.30	0.576	0.414	1.131	0.070
		0.569	0.418	1.075	0.073
		0.564	0.405	1.144	0.067
		0.571	0.423	1.075	0.073
		0.569	0.411	1.133	0.068
		0.570	0.421	1.077	0.072
	0.41	0.370	0.283	0.818	0.067
		0.366	0.276	0.864	0.063

		0.367	0.276	0.860	0.064
		0.370	0.286	0.829	0.066
		0.376	0.291	0.785	0.072
		0.371	0.291	0.794	0.071
	0.52	0.249	0.200	0.571	0.065
		0.248	0.199	0.610	0.060
		0.247	0.198	0.596	0.065
		0.249	0.200	0.613	0.065
		0.250	0.199	0.656	0.059
		0.250	0.199	0.646	0.057
	0.58	0.199	0.161	0.572	0.051
		0.200	0.162	0.536	0.059
		0.200	0.165	0.468	0.067
		0.203	0.164	0.616	0.049
		0.203	0.166	0.517	0.061
	0.71	0.147	0.122	0.493	0.047
		0.146	0.123	0.623	0.028
		0.145	0.122	0.603	0.032
		0.149	0.125	0.539	0.039
		0.149	0.124	0.585	0.035
	0.80	0.127	0.108	0.355	0.055
		0.125	0.107	0.350	0.054
		0.123	0.105	0.485	0.029
		0.125	0.106	0.397	0.043
4e	0.79	0.095	0.083	0.408	0.039
		0.093	0.081	0.423	0.036
		0.090	0.079	0.404	0.034
4f	0.05	1.970	0.956	2.587	0.069
		1.984	0.966	2.617	0.067
		1.986	0.945	2.631	0.060

0.10	1.211	0.664	2.031	0.065
	1.244	0.695	2.052	0.068
	1.238	0.684	2.088	0.056
0.20	0.606	0.388	1.470	0.050
	0.634	0.400	1.378	0.067
	0.594	0.399	1.419	0.048
0.31	0.342	0.241	0.981	0.055
	0.350	0.248	1.163	0.039
	0.349	0.237	0.831	0.053
	0.326	0.243	1.055	0.031
0.39	0.226	0.174	0.718	0.053
	0.226	0.175	0.845	0.038
	0.210	0.165	0.800	0.023
0.52	0.147	0.122	0.664	0.032
	0.146	0.122	0.641	0.038
	0.139	0.116	0.622	0.017
0.60	0.116	0.098	0.526	0.041
	0.113	0.097	0.534	0.039
	0.108	0.091	0.496	0.019
0.70	0.096	0.084	0.452	0.043
	0.093	0.081	0.431	0.046
	0.093	0.082	0.433	0.046
	0.091	0.079	0.414	0.024
	0.090	0.079	0.418	0.026
	0.092	0.080	0.426	0.024
	0.093	0.081	0.431	0.023
0.80	0.076	0.067	0.361	0.045
	0.074	0.066	0.342	0.046
	0.074	0.066	0.350	0.048
	0.072	0.063	0.339	0.047

0.073	0.064	0.335	0.047
0.074	0.065	0.349	0.046

Plots of single and two component exponential fits obtained in relaxation analyses of mixtures including ionic liquids 4a-d,f
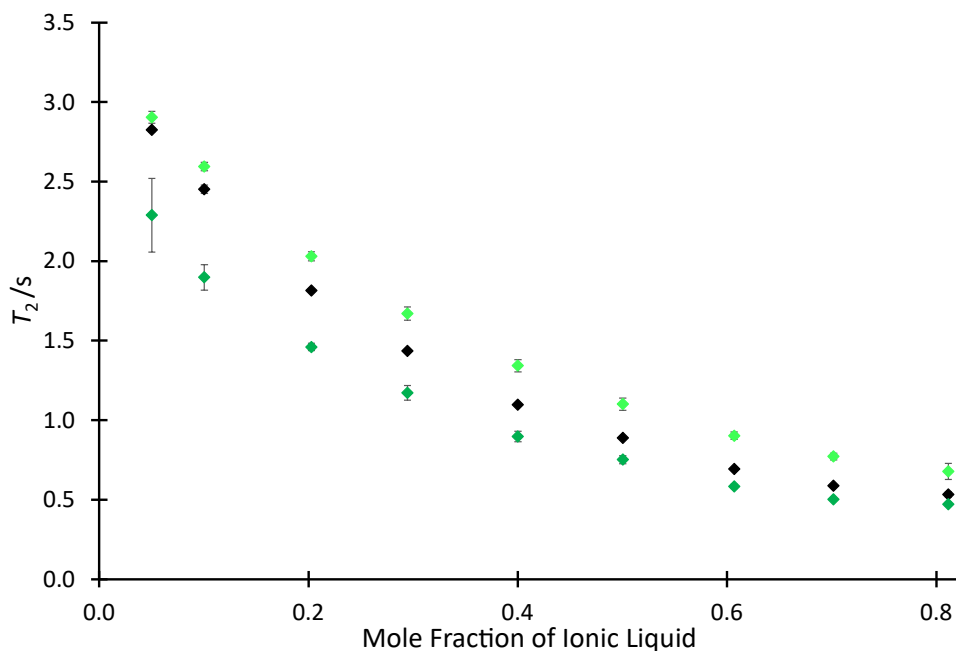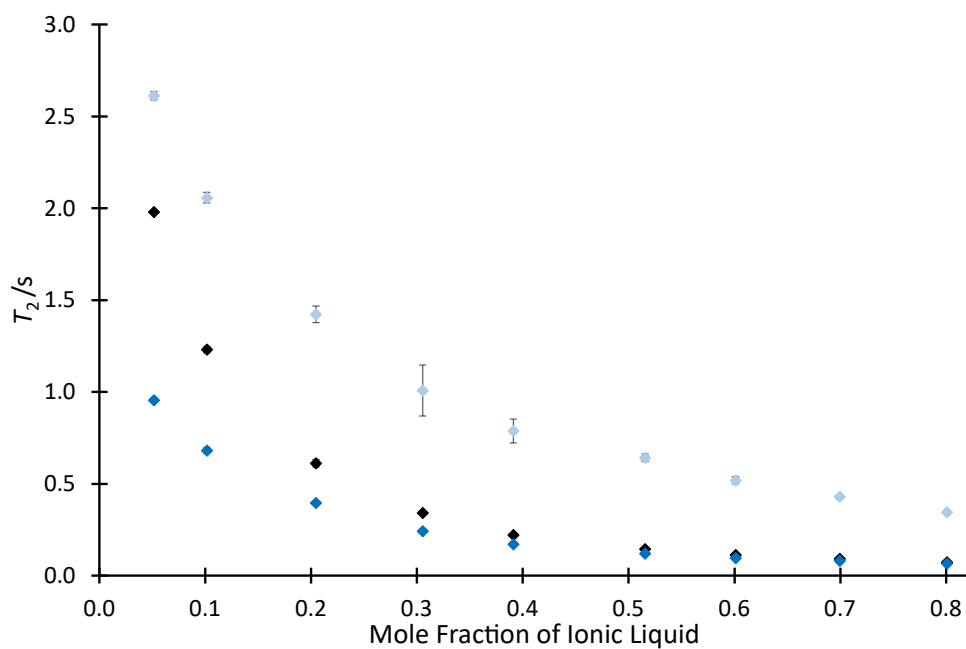

Figure S5. The spin-spin relaxation times associated with fitting either a single-component exponential (T_2, ◆) or two-component exponential ($T_{2(IL)}$, ◆, and $T_{2(non-IL)}$, ◆) for mixtures of [C_2C_1im][$N(SO_2CF_3)_2$] **4a**, pyridine **2** and acetonitrile. Uncertainties are reported as the standard deviation of at least triplicate results. Some uncertainties fall within the size of the markers used.
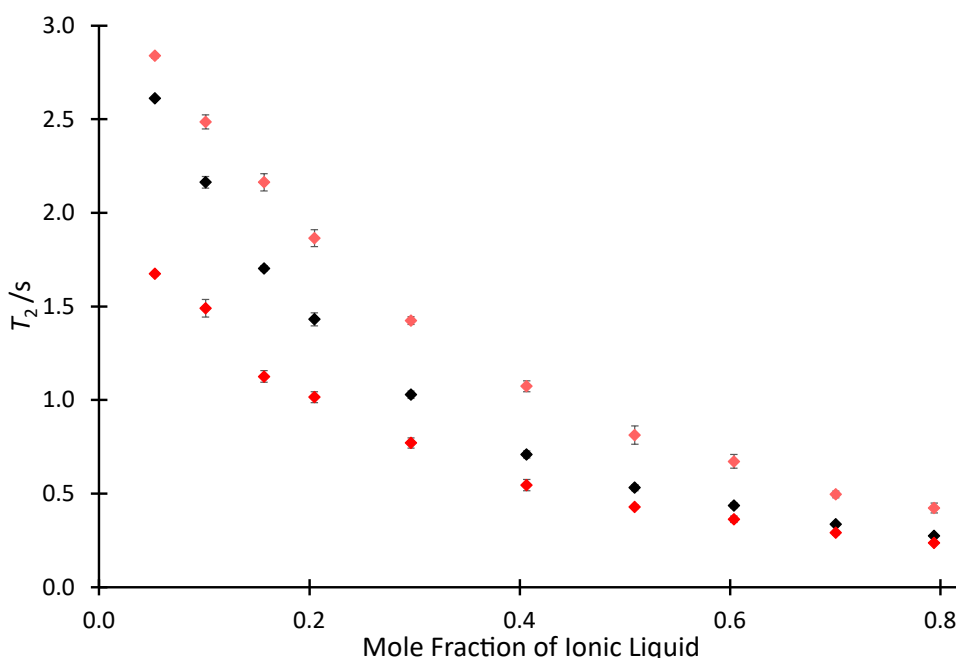
Figure S6. The spin-spin relaxation times associated with fitting either a single-component exponential (T_2, ◆) or two-component exponential ($T_{2(IL)}$, ◆, and $T_{2(non-IL)}$, ◆) for mixtures of [C_4C_1im][$N(SO_2CF_3)_2$] **4b**, pyridine **2** and acetonitrile. Uncertainties are reported as the standard deviation of at least triplicate results. Some uncertainties fall within the size of the markers used.
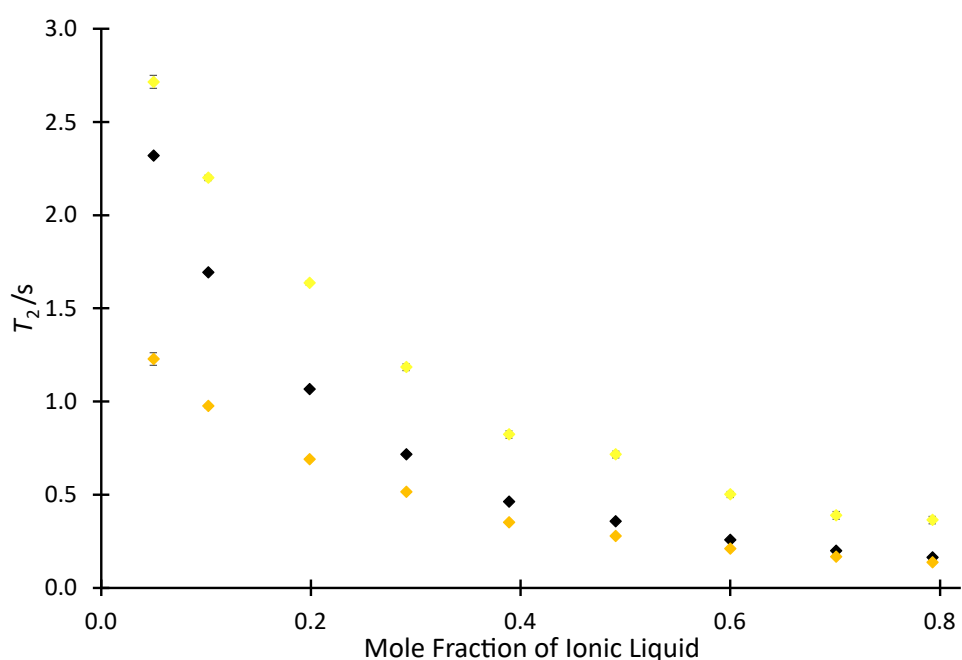
Figure S7. The spin-spin relaxation times associated with fitting either a single-component exponential (T_2, ◆) or two-component exponential ($T_{2(IL)}$, ◆, and $T_{2(non-IL)}$, ◆) for mixtures of [C_6C_1im][$N(SO_2CF_3)_2$] **4c**, pyridine **2** and acetonitrile. Uncertainties are reported as the standard deviation of at least triplicate results. Some uncertainties fall within the size of the markers used.
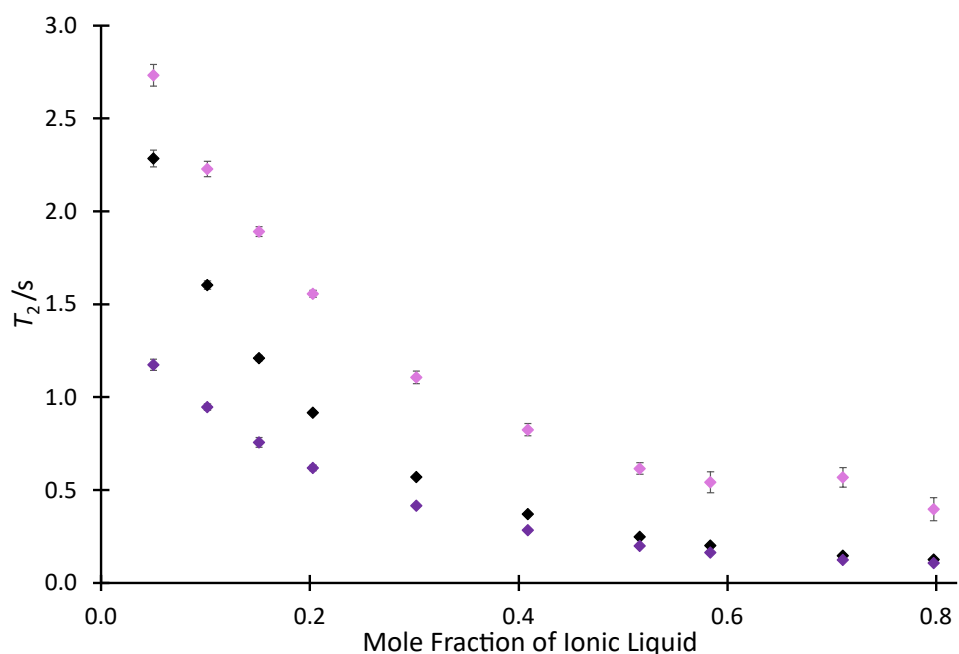
Figure S8. The spin-spin relaxation times associated with fitting either a single-component exponential (T_2, ◆) or two-component exponential ($T_{2(IL)}$, ◆, and $T_{2(non-IL)}$, ◆) for mixtures of [C_8C_1im][$N(SO_2CF_3)_2$] **4d**, pyridine **2** and acetonitrile. Uncertainties are reported as the standard deviation of at least triplicate results. Some uncertainties fall within the size of the markers used.

Figure S9. The spin-spin relaxation times associated with fitting either a single-component exponential (T_2, ◆) or two-component exponential ($T_{2(IL)}$, ◆, and $T_{2(non-IL)}$, ◆) for mixtures of [$C_{12}C_1$im][N(SO$_2$CF$_3$)$_2$] **4f**, pyridine **2** and acetonitrile. Uncertainties are reported as the standard deviation of at least triplicate results. Some uncertainties fall within the size of the markers used.

Analysis of the relaxation times (T₂) as a function of ionic liquid cation

It is of interest to consider how the relaxation time changes with the nature of the ionic liquid cation. The data at χ_{IL} *ca.* 0.8 was analysed using a power law (as has been done previously for relaxation times of simple alkanes in different mixtures[6])

$$\frac{T_{2(IL)}(IL_A)}{T_{2(IL)}(IL_B)} = \left(\frac{N(IL_A)}{N(IL_B)}\right)^x$$

where *N* was used to indicate the change in the length of the alkyl chain on the tail.

Analysis using *N* as the total number of heavy atoms in the cation of the ionic liquid and normalising to the ionic liquid **4a** (using it for IL$_B$) gave a poor fit and noticeable systematic deviation (Figure S10 below, which is the linear form of the equation above). In contrast, using *N* as the number of carbon atoms in the alkyl chain gave an excellent fit and a value of *x* of -1.11 $\pm$ 0.02 (Figure S11 below, also in the linear form). This comparison suggests that it is the change in the length of the alkyl tail and associated changes in structuring that are responsible for the changes in observed relaxation times.
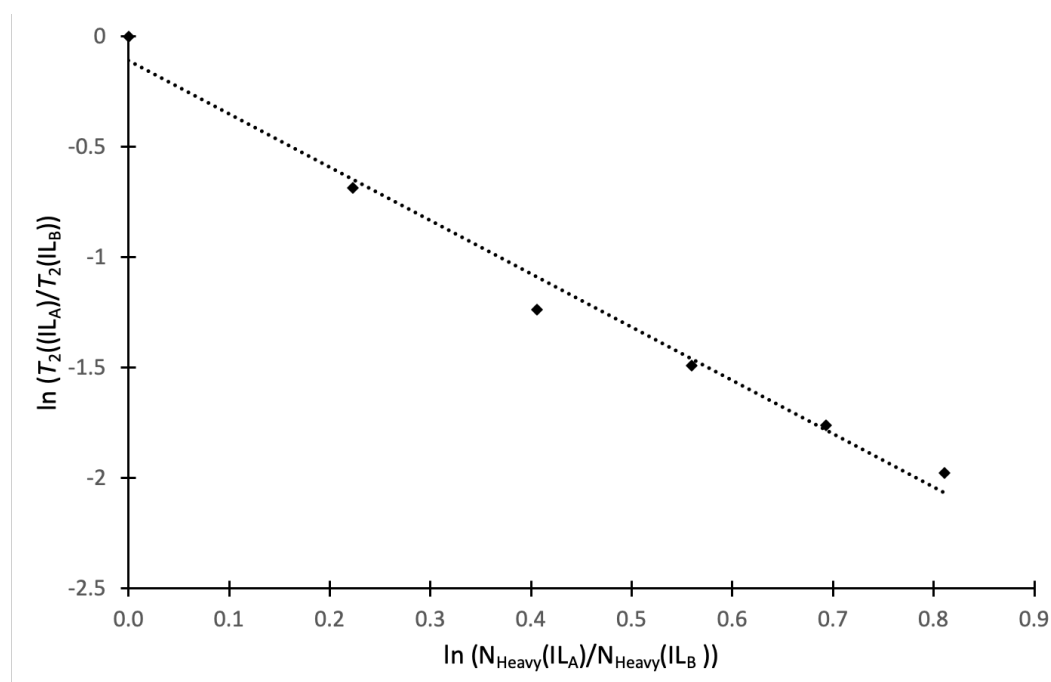
Figure S10. Plot of the log of the normalised relaxation times for the ionic liquid component (χ_{IL} *ca*. 0.8) against the log of the normalised number of heavy atoms in the cation; in this case IL$_B$ is the ethyl derivative **4a**.
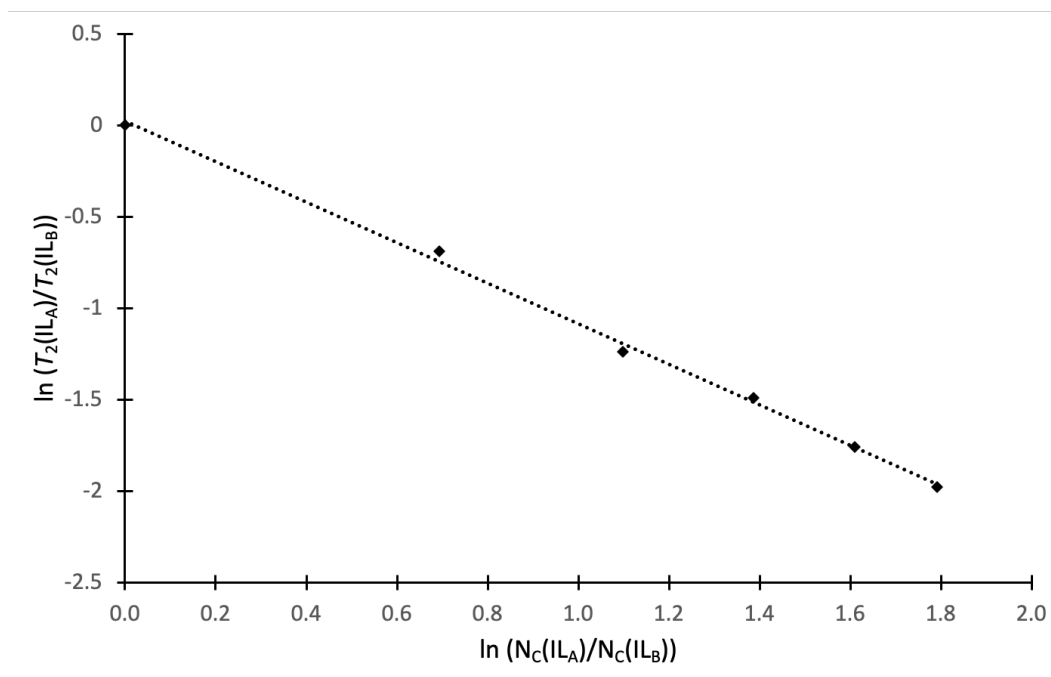
Figure S11. Plot of the log of the normalised relaxation times for the ionic liquid component (χ_{IL} *ca*. 0.8) against the log of the normalised number of carbon atoms in the alkyl chain on the cation; in this case IL_B is the ethyl derivative **4a**.

A similar argument can be constructed to examine the effect of changing the proportion of ionic liquid in the reaction mixture. The ratio of any two relaxation times,

$$\frac{T_{2(\text{IL})}(\text{IL}_A)}{T_{2(\text{IL})}(\text{IL}_B)}$$

would be expected to remain constant across different solvent compositions, unless the ordering in solution changed more in one case than another. By plotting this ratio for each of the ionic liquids **4b,c,d,f** (IL_A) with respect to the shortest chain case (that is, setting IL_B as **4a**) where the least structuring in solution would be expected, several points are clear (plotted in the log form as Figure S12).

   i)   There is a decrease in the ratio with increasing proportion of ionic liquid in the reaction mixture in each case, suggesting there is greater structuring at higher proportions of ionic liquid.[*]

   ii)   This effect becomes greater with longer alkyl chains.

---

[*] This argument works on the basis that there is minimal ordering in the case of the ethyl derivative **4a**; if there is any ordering, the argument is further enhanced.

41

iii)   There is a marked change in the effect between the hexyl and octyl systems (**4c** and **4d**) consistent with the argument presented that there is notable structural change between those two cases.
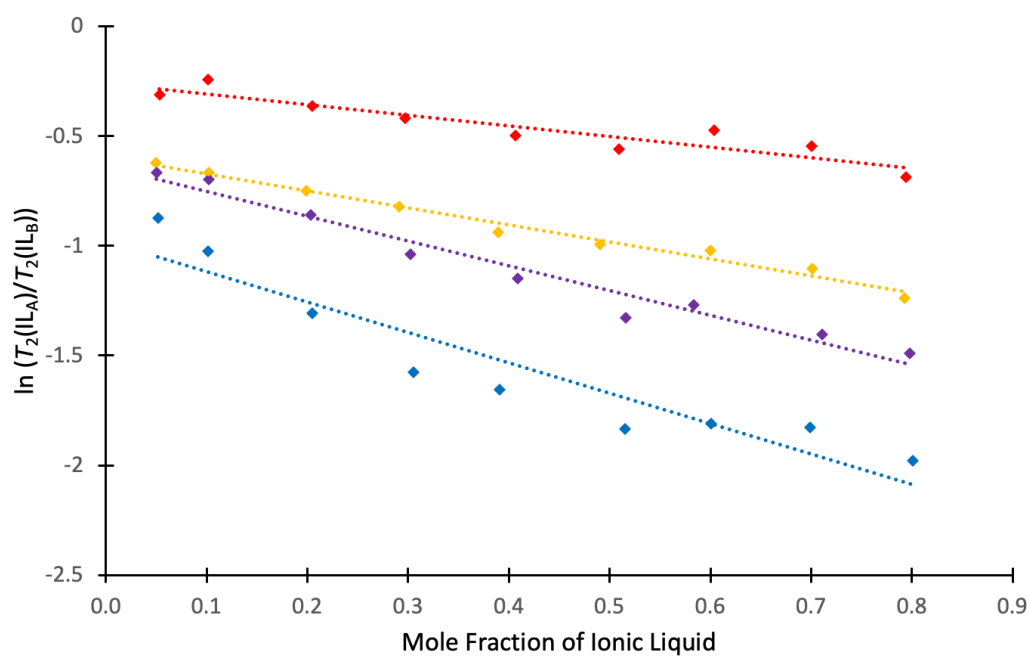
Figure S12. Plot of the log of the normalised relaxation times for the ionic liquid component across different proportions of the ionic liquids in acetonitrile for the ionic liquids $[C_4C_1im][N(SO_2CF_3)_2]$ **4b** (◆), $[C_6C_1im][N(SO_2CF_3)_2]$ **4c** (◆), $[C_8C_1im][N(SO_2CF_3)_2]$ **4d** (◆) and $[C_{12}C_1im][N(SO_2CF_3)_2]$ **4f** (◆) (IL$_A$) normalised against the ethyl derivative **4a** (IL$_B$). Lines are included for indicative purposes only and have no physical meaning.

Analysis of the relaxation times (Τ₂) as a function of amount of ionic liquid in the mixture

It has been shown that, with increasing volume fraction in the mixture, a transition occurs from 'ionic liquid dissolved in acetonitrile' to 'acetonitrile dissolved in ionic liquid'.[7] The proportion of ionic liquid at which there are equal volumes of each solvent present can be estimated based on molar volumes (assuming negligible volume of mixing) and occur at χ_{IL} *ca.* 0.16 for salt **4a**, χ_{IL} *ca.* 0.15 for salt **4b**, χ_{IL} *ca.* 0.14 for salt **4c**, χ_{IL} *ca.* 0.13 for salt **4d** and χ_{IL} *ca.* 0.11 for salt **4e**.

The data presented in the manuscript in Figure 5 suggests a change in the nature of the solution, as indicated by the slope of the plot of $1/T_2$ against mole fraction of ionic liquid in the reaction mixture. The change in slope is demonstrated in Figures S13, where tangents are taken at the extremes of the mole fraction plot. With the exception of the ethyl case **4a** (which is effectively linear), all others show a change in slope consistent with a change in the nature of solvation; in the case of salt **4a** either there is little change in the nature of the solution or the effects of each 'dominant' solvent are similar. It should be noted that the intercept of the two tangents generally move to lower mole fraction with increasing alkyl chain length, consistent with the solvent transition happening at lower mole fraction. This argument is consistent with the volume fraction argument above, noting that the values determined from the plots are systematically higher.
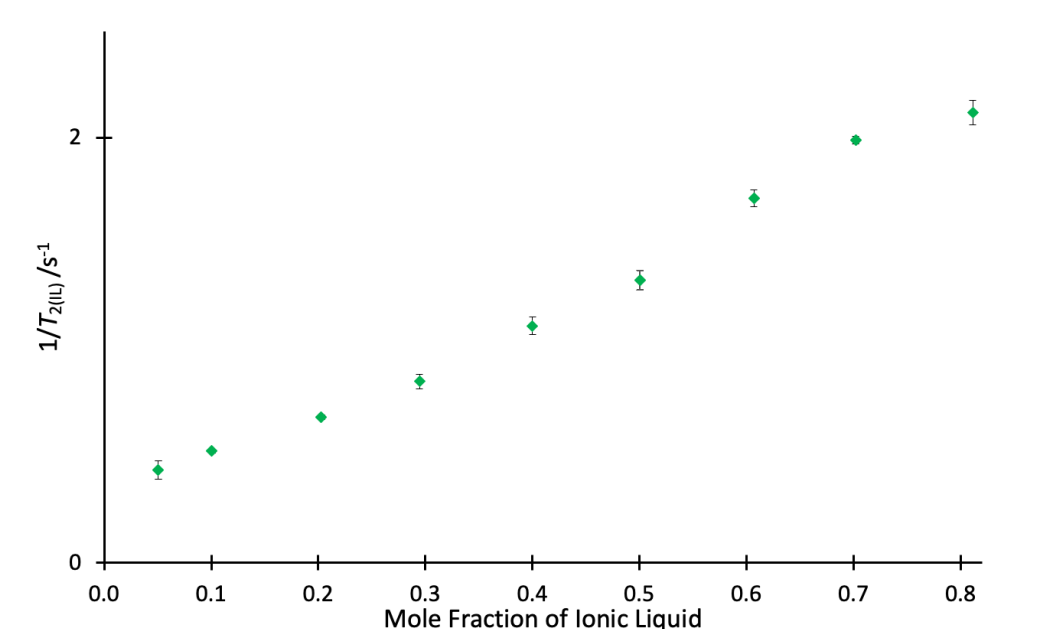
Figure S13. The reciprocal of spin-spin relaxation time for the ionic liquid component ($1/T_{2(IL)}$) in mixtures containing different proportions of [C₂C₁im][N(SO₂CF₃)₂] **4a** (◆) in acetonitrile. Uncertainties are reported as the standard deviation of at least triplicate results. Some uncertainties fall within the size of the markers used.
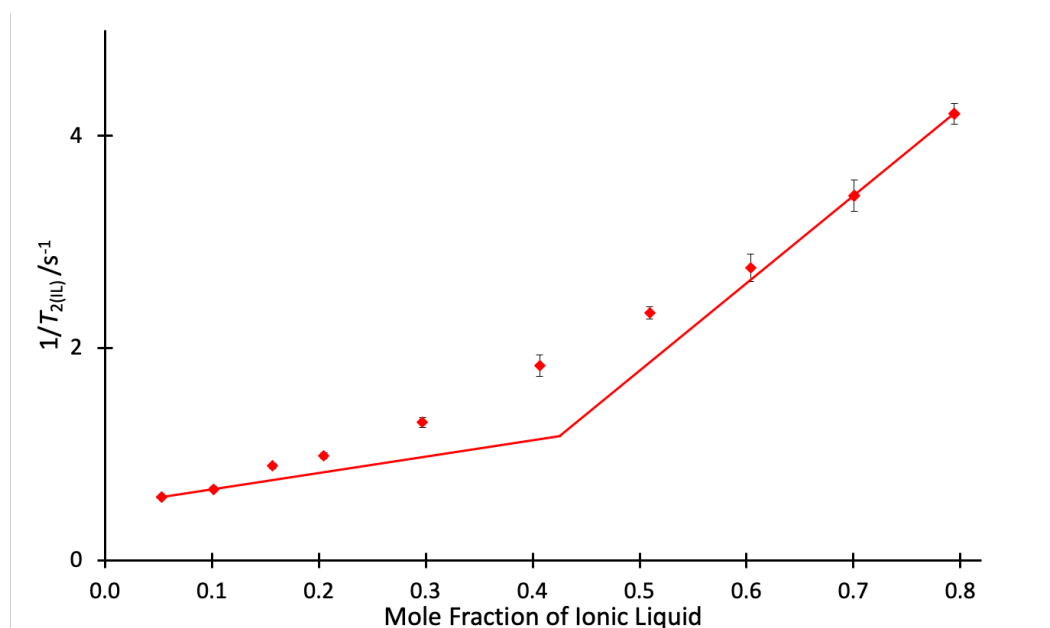
Figure S14. The reciprocal of spin-spin relaxation time for the ionic liquid component ($1/T_{2(IL)}$) in mixtures containing different proportions of $[C_4C_1im][N(SO_2CF_3)_2]$ **4b** (◆) in acetonitrile. Uncertainties are reported as the standard deviation of at least triplicate results. Some uncertainties fall within the size of the markers used. Lines have been added to guide the eye and give an indication of the changing slope of the data.
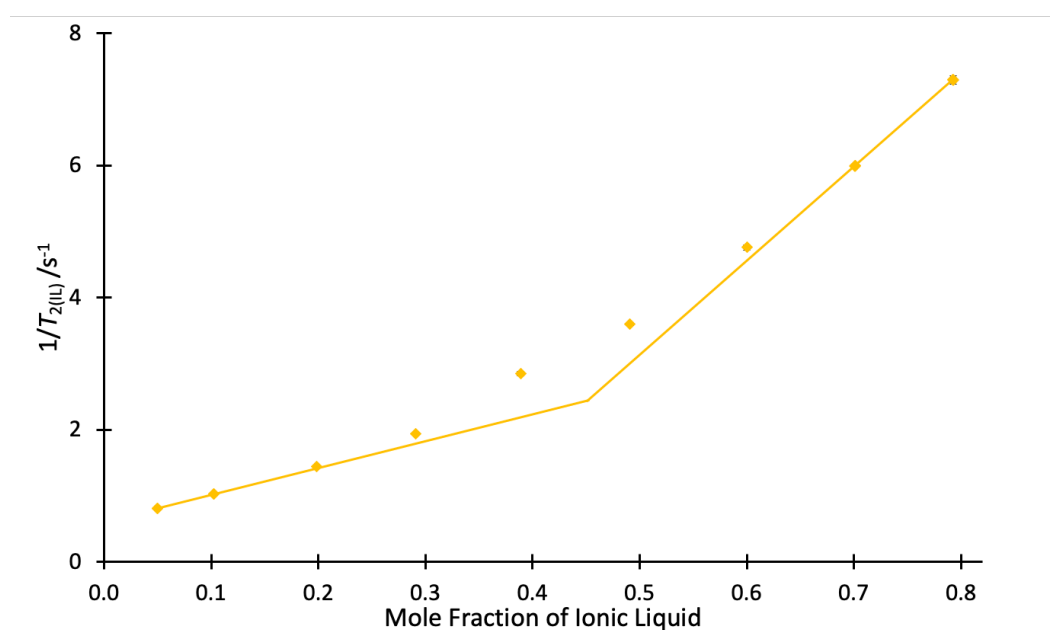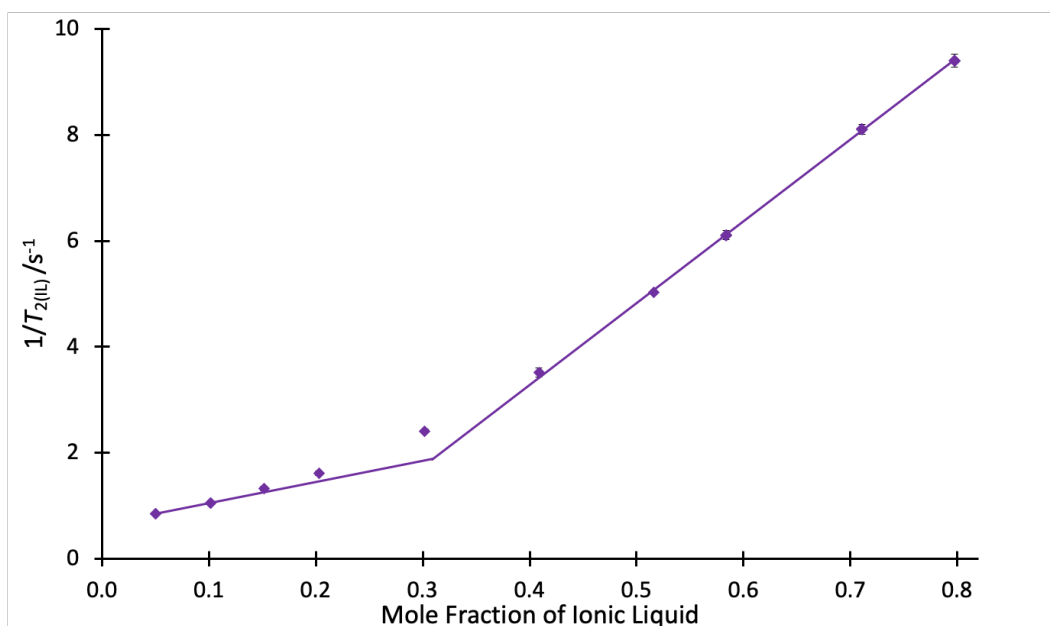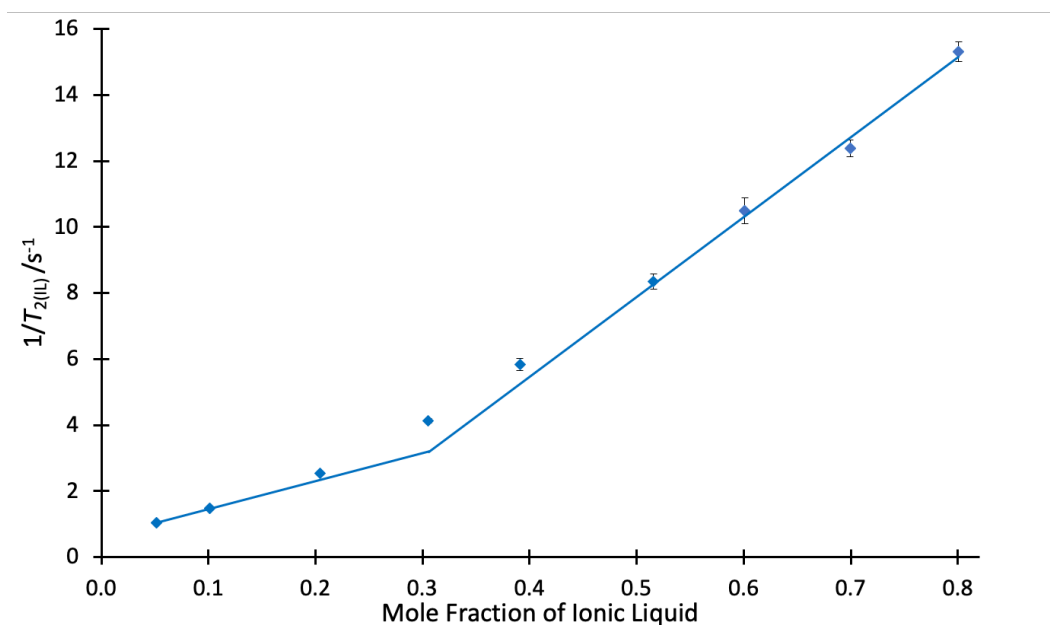

Figure S15. The reciprocal of spin-spin relaxation time for the ionic liquid component ($1/T_{2(IL)}$) in mixtures containing different proportions of $[C_6C_1im][N(SO_2CF_3)_2]$ **4c** (◆) in acetonitrile. Uncertainties are reported as the standard deviation of at least triplicate results. Some uncertainties fall within the size of the markers used. Lines have been added to guide the eye and give an indication of the changing slope of the data.

Figure S16. The reciprocal of spin-spin relaxation time for the ionic liquid component ($1/T_{2(IL)}$) in mixtures containing different proportions of $[C_8C_1im][N(SO_2CF_3)_2]$ **4d** ($\blacklozenge$) in acetonitrile. Uncertainties are reported as the standard deviation of at least triplicate results. Some uncertainties fall within the size of the markers used. Lines have been added to guide the eye and give an indication of the changing slope of the data.

Figure S17. The reciprocal of spin-spin relaxation time for the ionic liquid component ($1/T_{2(IL)}$) in mixtures containing different proportions of $[C_{12}C_1im][N(SO_2CF_3)_2]$ **4f** ($\blacklozenge$) in acetonitrile. Uncertainties are reported as the standard deviation of at least triplicate results. Some uncertainties fall within the size of the markers used. Lines have been added to guide the eye and give an indication of the changing slope of the data.

Initially considered correlations of k_2 and T_2

In considering the k_2 and T_2 data, several relationships were initially considered and they are shown below. It is important to note that these Figures are included to particularly emphasise that there is not a straightforward relationship between the data as presented and to justify the use of the more complicated relationships shown in Figures 6 and 7 in the main text. Lines are included to guide the eye only and to demonstrate that, in fact, there are no simple linear relationships between the properties as drawn.
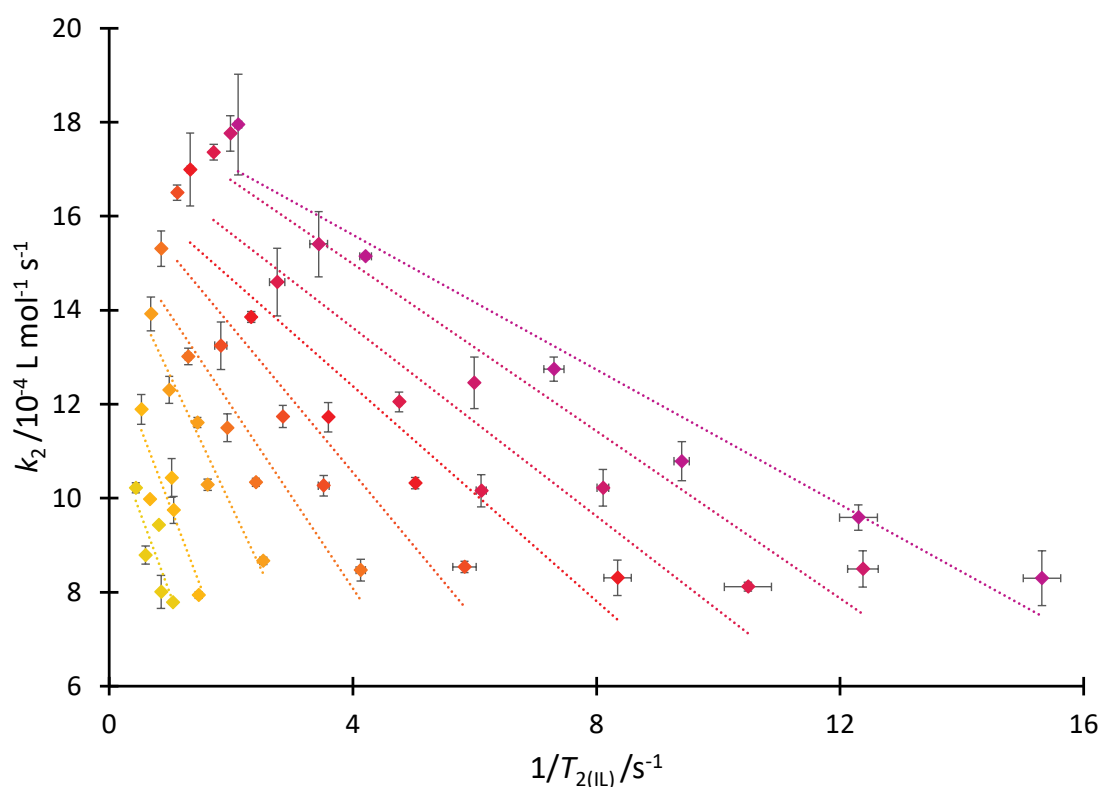
Figure S18. Correlation of the bimolecular rate coefficient (k_2) for the reaction of benzyl bromide **1** and pyridine **2** with the reciprocal of spin-spin relaxation time for the ionic liquid component ($1/T_{2(IL)}$) in mixtures containing each of the ionic liquids **4a-d,f** at constant mole fractions of ionic liquid, χ_{IL} *ca.* 0.05 (◆), 0.1 (◆), 0.2 (◆), 0.3 (◆), 0.4 (◆), 0.5 (◆), 0.6 (◆), 0.7 (◆) or 0.8 (◆additionally includes salt **4e**). Uncertainties are reported as the standard deviation of at least triplicate results (k_2) or as the propagation of the standard deviation of at least triplicate results ($1/T_{2(IL)}$). Some uncertainties fall within the size of the markers used. Lines are presented to guide the eye only; there is no argument that a linear fit is appropriate here.
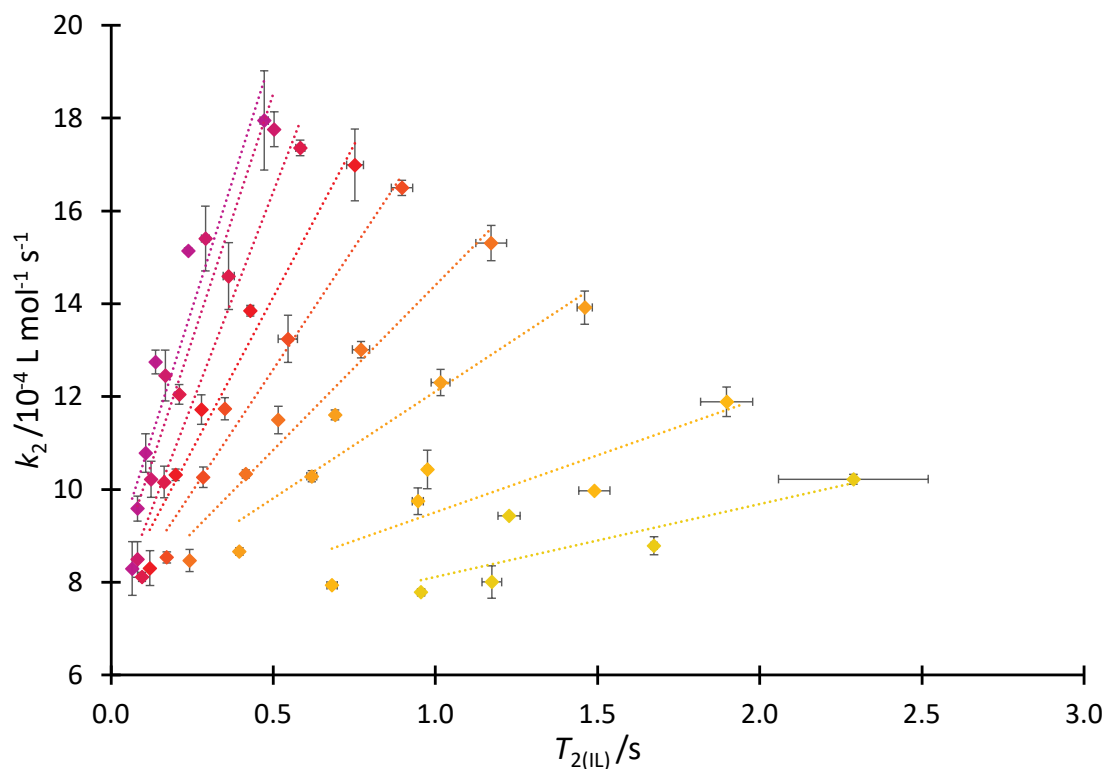
Figure S19. Correlation of the bimolecular rate coefficient (k_2) for the reaction of benzyl bromide **1** and pyridine **2** with the spin-spin relaxation time for the ionic liquid component ($T_{2(IL)}$) in mixtures containing each of the ionic liquids **4a-d,f** at constant mole fractions of ionic liquid, χ_{IL} *ca.* 0.05 (◆), 0.1 (◆), 0.2 (◆), 0.3 (◆), 0.4 (◆), 0.5 (◆), 0.6 (◆), 0.7 (◆) or 0.8 (◆additionally includes salt **4e**). Uncertainties are reported as the standard deviation of at least triplicate results. Some uncertainties fall within the size of the markers used. Lines are presented to guide the eye only; there is no argument that a linear fit is appropriate here.
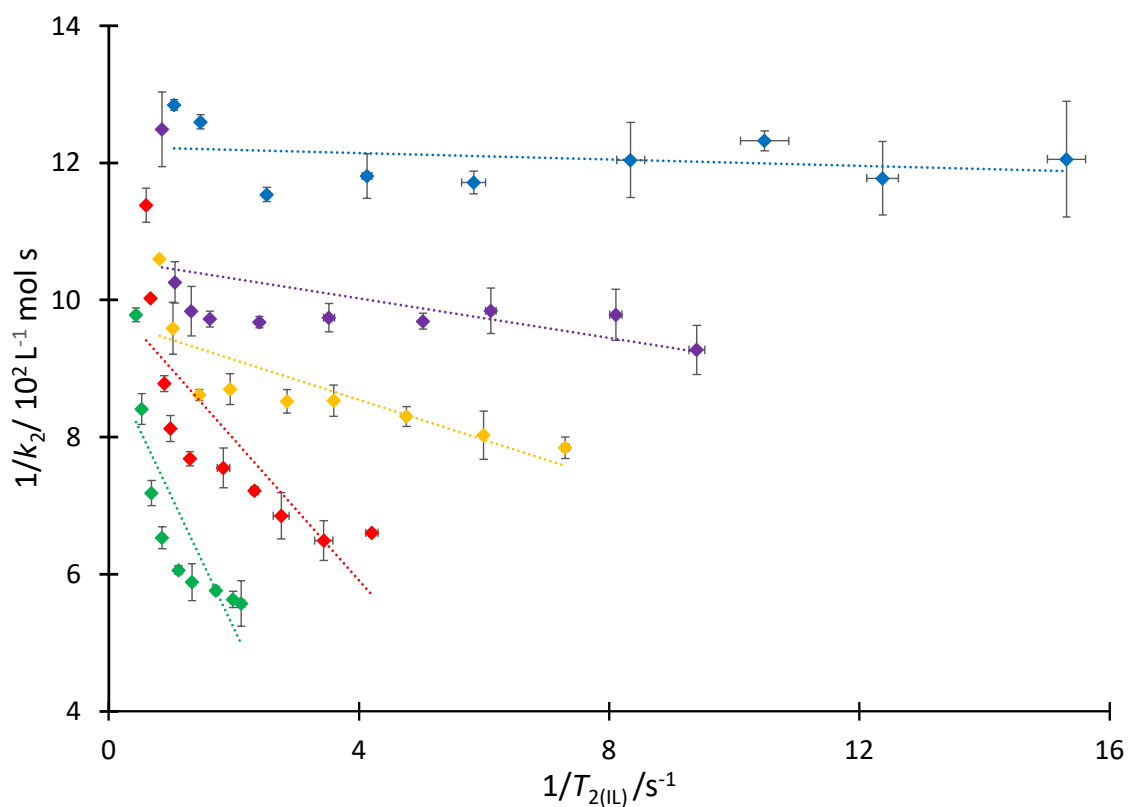
Figure S20. Correlation of the reciprocal of the bimolecular rate coefficient ($1/k_2$) for the reaction of benzyl bromide **1** and pyridine **2** with the reciprocal of spin-spin relaxation time for the ionic liquid component ($1/T_{2(IL)}$) in mixtures containing different proportions of either $[C_2C_1im][N(SO_2CF_3)_2]$ **4a** (◆), $[C_4C_1im][N(SO_2CF_3)_2]$ **4b** (◆),[8] $[C_6C_1im][N(SO_2CF_3)_2]$ **4c** (◆), $[C_8C_1im][N(SO_2CF_3)_2]$ **4d** (◆), or $[C_{12}C_1im][N(SO_2CF_3)_2]$ **4f** (◆) in acetonitrile. Uncertainties are reported as the propagation of the standard deviation of at least triplicate results. Some uncertainties fall within the size of the markers. Lines are presented to guide the eye only; there is no argument that a linear fit is appropriate here.
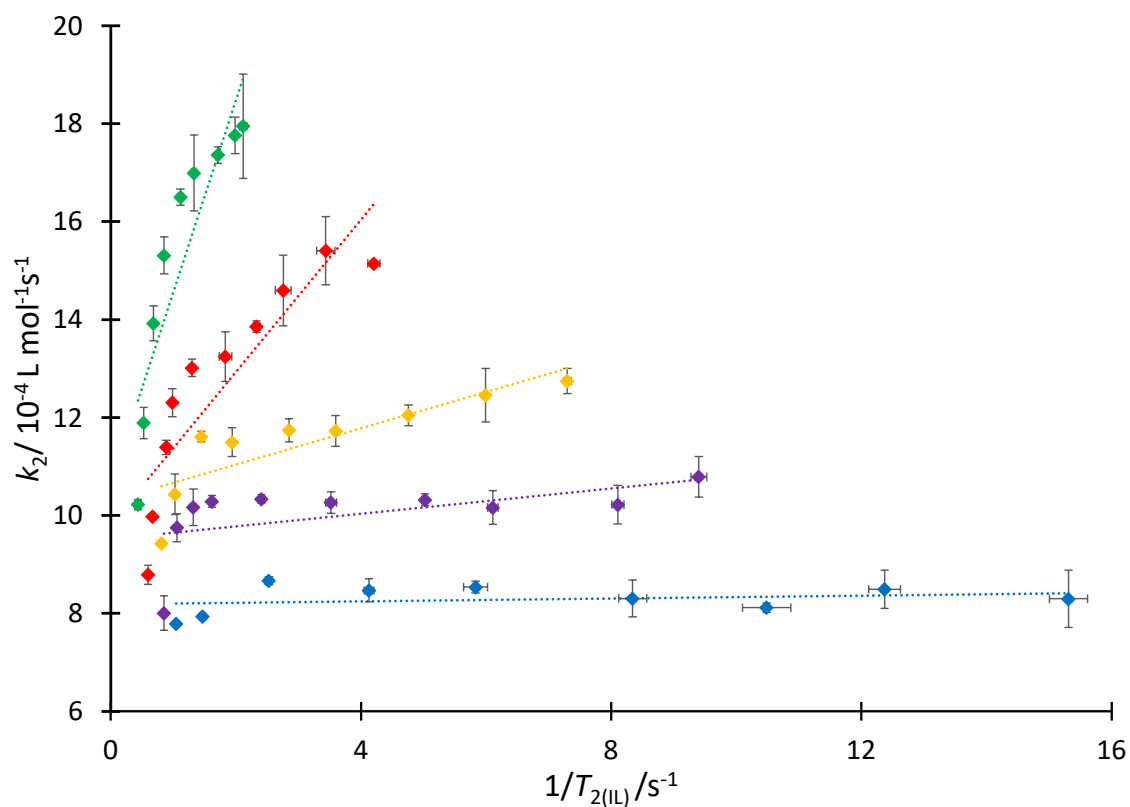
Figure S21. Correlation of the bimolecular rate coefficient (k_2) for the reaction of benzyl bromide **1** and pyridine **2** with the reciprocal of spin-spin relaxation time for the ionic liquid component ($1/T_{2(IL)}$) in mixtures containing different proportions of either [C_2C_1im][N(SO$_2$CF$_3$)$_2$] **4a** (◆), [C_4C_1im][N(SO$_2$CF$_3$)$_2$] **4b** (◆),[8] [C_6C_1im][N(SO$_2$CF$_3$)$_2$] **4c** (◆), [C_8C_1im][N(SO$_2$CF$_3$)$_2$] **4d** (◆), or [$C_{12}C_1$im][N(SO$_2$CF$_3$)$_2$] **4f** (◆) in acetonitrile. Uncertainties are reported as the propagation of the standard deviation of at least triplicate results. Some uncertainties fall within the size of the markers. Lines are presented to guide the eye only; there is no argument that a linear fit is appropriate here.

Exact compositions and associated fitting parameters for mixtures of salt 5 used in relaxation analyses

Table S17. Composition of stock solutions by mass, including resultant mole fraction, and associated splitting parameter, ϕ_{IL}, for the mole fraction dependent relaxation studies for mixtures of [BMMO][N(SO$_2$CF$_3$)$_2$] **5** and acetonitrile.

Mass salt **5** / g	Mass CH$_3$CN / g	Mass **2** / g	χ_5	ϕ_{IL}
0	1.531	0.081	0	-
0.137	0.290	0.016	0.04	0.2199
0.287	0.228	0.016	0.10	0.4255
0.357	0.189	0.016	0.15	0.5241
0.430	0.147	0.016	0.21	0.6254
0.522	0.103	0.011	0.31	0.7441
0.572	0.074	0.013	0.40	0.8072
0.609	0.056	0.010	0.48	0.8537
0.646	0.033	0.013	0.60	0.9006
0.672	0.023	0.011	0.69	0.9292

Mole fraction dependent relaxation data for salt 5

Table S18. The calculated single-component (T_2) and two-component ($T_{2(IL)}$ and $T_{2(non-IL)}$) exponential decay constants, as well as the noise fraction of signal, determined in the relaxation studies of mixtures of [C$_4$C$_1$mo][N(SO$_2$CF$_3$)$_2$] **5**, pyridine **2** and acetonitrile.

χ_5	T_2 / s	$T_{2(IL)}$ /s	$T_{2(non-IL)}$	Noise
0.04	2.474	1.266	2.890	0.069
	2.465	1.265	2.874	0.069
	2.464	1.249	2.877	0.067
	2.460	1.253	2.871	0.066
	2.465	1.239	2.882	0.066
	2.464	1.263	2.872	0.064
	2.463	1.261	2.872	0.066
0.10	1.610	0.886	2.397	0.069

	1.605	0.892	2.373	0.069
	1.608	0.889	2.387	0.067
	1.610	0.894	2.383	0.066
	1.611	0.886	2.396	0.067
	1.596	0.876	2.373	0.067
	1.607	0.882	2.393	0.067
0.15	1.198	0.698	2.062	0.069
	1.202	0.702	2.124	0.066
	1.212	0.704	2.106	0.066
	1.211	0.707	2.091	0.065
	1.207	0.700	2.098	0.063
	1.208	0.705	2.087	0.063
	1.210	0.701	2.105	0.060
0.21	0.792	0.491	1.657	0.066
	0.800	0.485	1.669	0.068
	0.801	0.485	1.694	0.067
	0.798	0.490	1.651	0.069
	0.791	0.484	1.700	0.063
	0.800	0.484	1.679	0.067
	0.797	0.488	1.683	0.066
0.31	0.407	0.271	1.134	0.067
	0.406	0.271	1.130	0.067
	0.409	0.272	1.149	0.064
	0.405	0.271	1.116	0.066
	0.405	0.273	1.093	0.067
	0.407	0.272	1.114	0.067
	0.406	0.273	1.104	0.066
0.40	0.232	0.172	0.829	0.062
	0.230	0.171	0.796	0.065
	0.232	0.172	0.849	0.061

|			
	0.231	0.170	0.859	0.061
	0.230	0.170	0.854	0.063
	0.231	0.171	0.809	0.066
	0.233	0.173	0.852	0.061
0.48	0.139	0.112	0.607	0.064
	0.144	0.113	0.561	0.066
	0.136	0.112	0.672	0.055
	0.137	0.113	0.654	0.057
	0.137	0.113	0.705	0.053
	0.138	0.113	0.700	0.054
	0.138	0.113	0.677	0.055
	0.138	0.114	0.683	0.054
0.60	0.073	0.062	0.353	0.064
	0.073	0.062	0.378	0.061
	0.073	0.063	0.358	0.064
	0.072	0.061	0.402	0.059
	0.073	0.062	0.410	0.060
	0.073	0.062	0.354	0.063
	0.072	0.062	0.382	0.062
0.69	0.048	0.043	0.278	0.061
	0.045	0.042	0.228	0.076
	0.048	0.043	0.299	0.062
	0.049	0.044	0.285	0.063
	0.049	0.043	0.287	0.062
	0.049	0.044	0.301	0.061
	0.048	0.043	0.291	0.062
	0.048	0.043	0.293	0.062
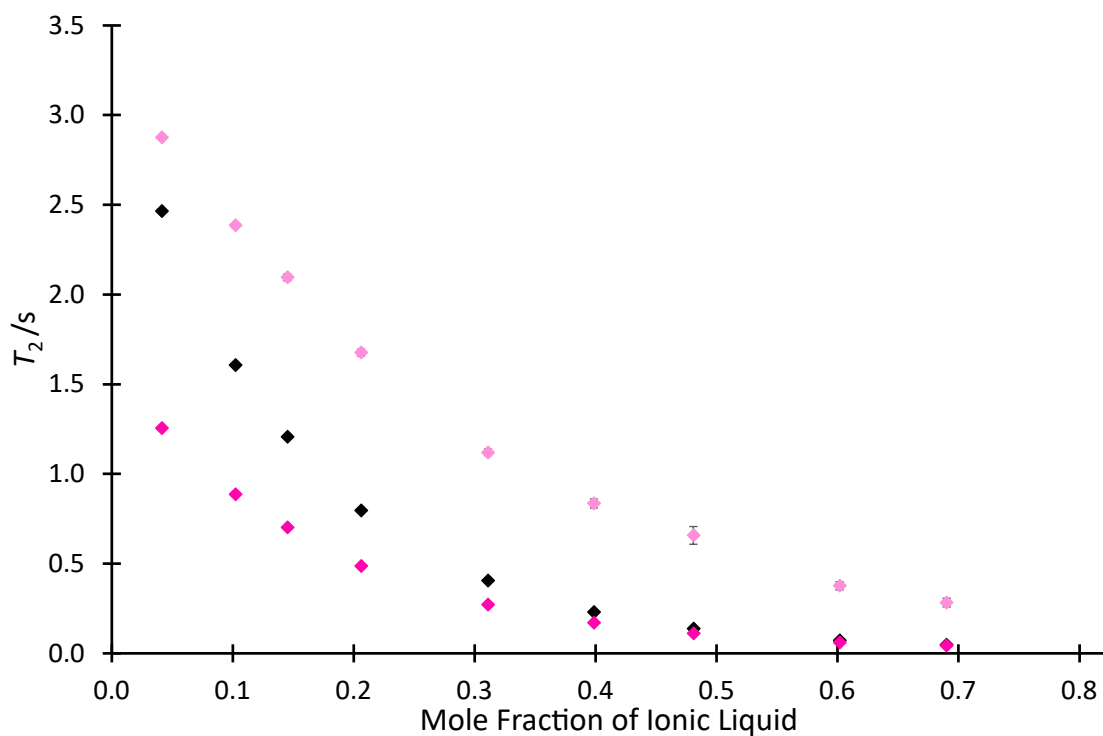
Figure S22. The spin-spin relaxation times associated with fitting either a single-component exponential (T_2, ◆) or two-component exponential ($T_{2(IL)}$, ◆, and $T_{2(non-IL)}$, ◆) for mixtures of [C$_4$C$_1$mo][N(SO$_2$CF$_3$)$_2$] **5**, pyridine **2** and acetonitrile. Uncertainties are reported as the standard deviation of at least triplicate results. Some uncertainties fall within the size of the markers used.

Methodology and results for predicting k$_2$ *in mixtures containing salt 5*

The values of k_2 and $T_{2\text{(non-IL)}}$ for the highest mole fraction of salt **5** investigated previously (χ_{IL} *ca*. 0.7)[9] was used along with the k_2 and T_2 data determined for neat acetonitrile to derive Equation 1, reproduced from the main text, below, which describes the straight line passing through these two points as a function of $T_{2\text{(non-IL)}}$.

$$k_{2\text{(predicted)}} = 3.40 \times 10^{-3} - 8.51 \times 10^{-4} \times T_{2\text{(non-IL)}}$$

Equation 1. The equation which was used to predict bimolecular rate coefficient data in systems containing salt **5**; $k_{2\text{(predicted)}}$ = the predicted bimolecular rate coefficient, $T_{2\text{(non-IL)}}$ = the spin-spin relaxation time of the non-ionic liquid component for each mixture.

The predicted rate coefficient data for salt **5** was then calculated using Equation S4 and the average $T_{2\text{(non-IL)}}$ associated with each mixture composition. It is worth noting, the non-ionic liquid spin-spin relaxation time was used such that the value of T_2 in neat acetonitrile (*i.e.* T_2 in the absence of any ionic liquid) could be used, hence performing the prediction by using only a single experimentally determined k_2 for this ionic liquid system.

Table S19. The predicted bimolecular rate coefficient ($k_{2(predicted)}$) and corresponding rate coefficient determined experimentally ($k_{2(experimental)}$, reproduced from Hawker *et al.*[9]) associated with the reaction of benzyl bromide **1** and pyridine **2** at 22.2°C in mixtures containing different proportions of $[C_4C_1mo][N(SO_2CF_3)_2]$ **5** in acetonitrile, as well as the spin-spin relaxation time of the non-ionic liquid component ($T_{2(non-IL)}$) used for calculation of the predicted data. Experimentally determined k_2 and T_2 for neat acetonitrile with pyridine **2** that was used for prediction is also included.

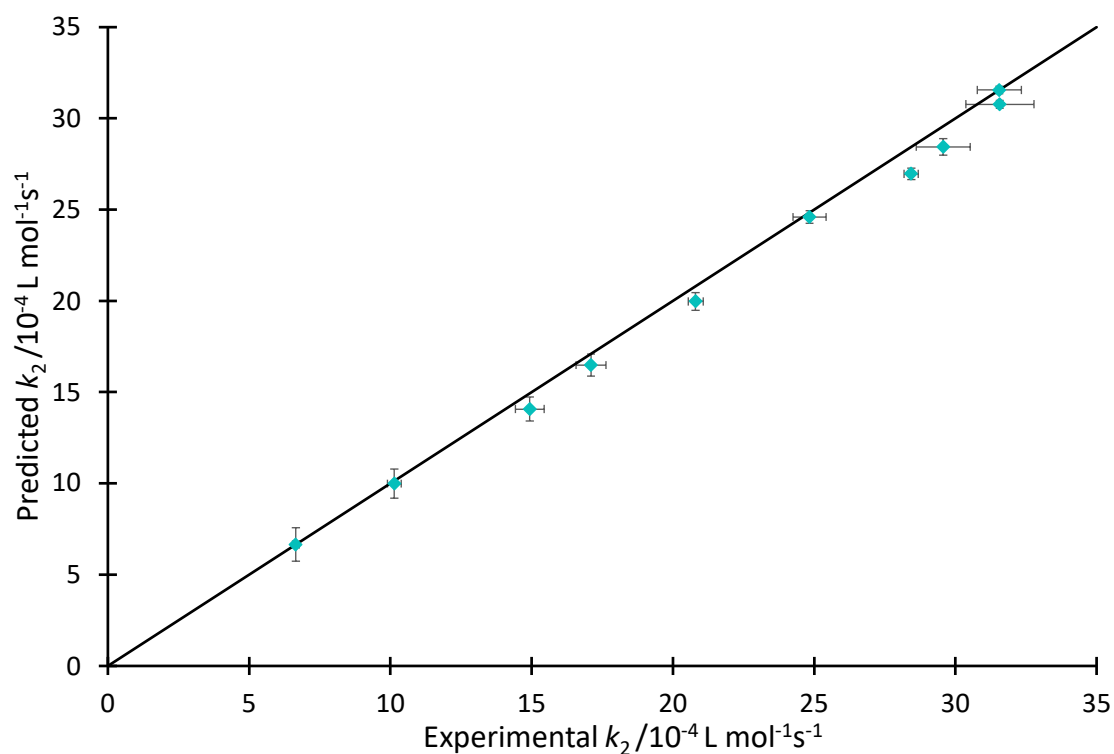| χ_5	$T_{2(non-IL)}$ /s	$k_{2(predicted)}$ / 10^{-4} L mol^{-1} s^{-1}	$k_{2(experimental)}$ / 10^{-4} L mol^{-1} s^{-1}
0	3.278	6.65	6.65
0.04	2.714	9.99	10.1
0.10	2.030	14.1	14.9
0.15	1.624	16.5	17.1
0.21	1.086	20.0	20.8
0.31	0.616	24.6	24.8
0.40	0.362	27.0	28.4
0.48	0.215	28.4	29.6
0.60	0.114	30.8	31.6
0.69	0.075	31.6	31.6

Figure S23. Comparison of the value of the bimolecular rate coefficient (k_2) for the reaction of benzyl bromide **1** and pyridine **2** in mixtures of [BMMO][N(SO$_2$CF$_3$)$_2$] **5** in acetonitrile, reproduced from Hawker *et al.*,[9] with the predicted values of k_2, calculated using the spin-spin relaxation time associated with the non-ionic liquid portion ($T_{2(non-IL)}$) of mixtures with the same compositions (◆). Uncertainties are reported as either the standard deviation of replicate results (experimental k_2) or the propagation of uncertainties associated with each of the two points used to form the prediction equation as well as the individual $T_{2(non-IL)}$ value used in calculation of each point (predicted k_2). Line shown is $y = x$, added as a guide only.

Representative viscosity data

It is expected that the viscosity of the mixtures would increase with the proportion of ionic liquid present; this feature was observed for the systems considered herein and a representative example is shown in Figure S24 for the octyl substituted system **4d**. It is important to note that the viscosity is not sufficient to explain the changes in the rate coefficient (not in the diffusion controlled regime; in fact, more viscous systems result in a greater rate coefficient).
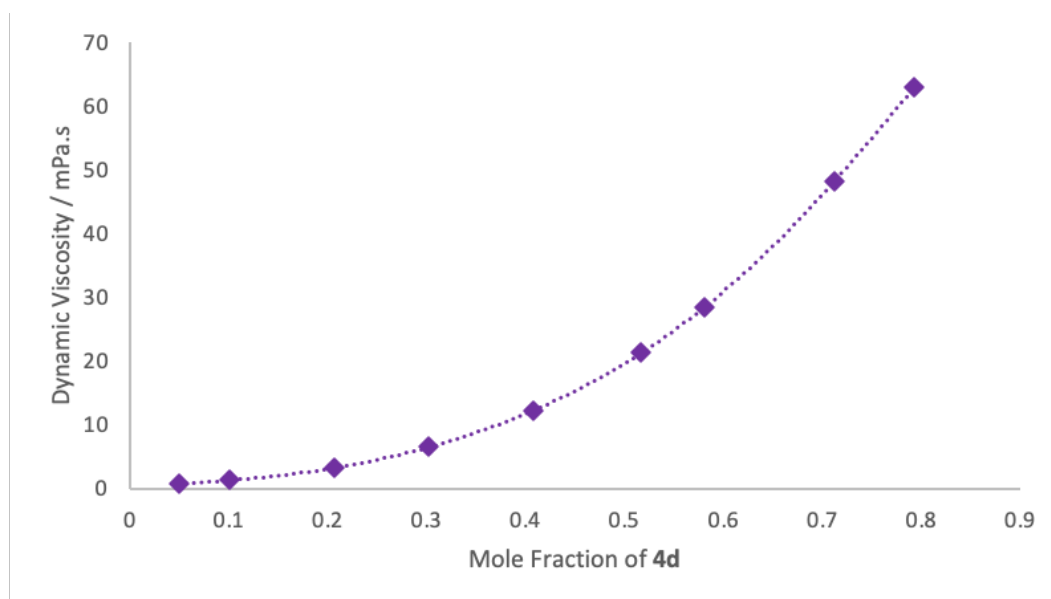

Figure S24. The dynamic viscosity of mixtures containing varying proportions of the ionic liquid **4d** in acetonitrile at 22.2°C. Uncertainties lie with the markers used. The line is added to guide the eye only.

References

1. T. Brünig, K. Krekić, C. Bruhn and R. Pietschnig, *Chem. Eur. J.*, 2016, **22**, 16200–16212.
2. S. Chakraborty, K. Jähnichen, H. Komber, A. A. Basfar and B. Voit, *Macromolecules*, 2014, **47**, 4186-4198.
3. Z.-B. Zhou, H. Matsumoto and K. Tatsumi, *Chem. Eur. J.*, 2006, **12**, 2196-2212.
4. P. Virtanen, R. Gommers, T. E. Oliphant, M. Haberland, T. Reddy, D. Cournapeau, E. Burovski, P. Peterson, W. Weckesser, J. Bright, S. J. van der Walt, M. Brett, J. Wilson, K. J. Millman, N. Mayorov, A. R. J. Nelson, E. Jones, R. Kern, E. Larson, C. J. Carey, İ. Polat, Y. Feng, E. W. Moore, J. VanderPlas, D. Laxalde, J. Perktold, R. Cimrman, I. Henriksen, E. A. Quintero, C. R. Harris, A. M. Archibald, A. H. Ribeiro, F. Pedregosa, P. van Mulbregt, A. Vijaykumar, A. P. Bardelli, A. Rothberg, A. Hilboll, A. Kloeckner, A. Scopatz, A. Lee, A. Rokem, C. N. Woods, C. Fulton, C. Masson, C. Häggström, C. Fitzgerald, D. A. Nicholson, D. R. Hagen, D. V. Pasechnik, E. Olivetti, E. Martin, E. Wieser, F. Silva, F. Lenders, F. Wilhelm, G. Young, G. A. Price, G.-L. Ingold, G. E. Allen, G. R. Lee, H. Audren, I. Probst, J. P. Dietrich, J. Silterra, J. T. Webber, J. Slavič, J. Nothman, J. Buchner, J. Kulick, J. L. Schönberger, J. V. de Miranda Cardoso, J. Reimer, J. Harrington, J. L. C. Rodríguez, J. Nunez-Iglesias, J. Kuczynski, K. Tritz, M. Thoma, M. Newville, M. Kümmerer, M. Bolingbroke, M. Tartre, M. Pak, N. J. Smith, N. Nowaczyk, N. Shebanov, O. Pavlyk, P. A. Brodtkorb, P. Lee, R. T. McGibbon, R. Feldbauer, S. Lewis, S. Tygier, S. Sievert, S. Vigna, S. Peterson, S. More, T. Pudlik, T. Oshima, T. J. Pingel, T. P. Robitaille, T. Spura, T. R. Jones, T. Cera, T. Leslie, T. Zito, T. Krauss, U. Upadhyay, Y. O. Halchenko, Y. Vázquez-Baeza and SciPy Contributors, *Nature Methods*, 2020, **17**, 261-272.
5. M. R. Gyton, M. L. Cole and J. B. Harper, *Chem. Commun.*, 2011, **47**, 9200-9202.
6. D. E. Freed, *J. Chem. Phys.*, 2007, **126**, 174502.
7. S. T. Keaveney, T. L. Greaves, D. F. Kennedy and J. B. Harper, *J. Phys. Chem. B*, 2016, **120**, 12687-12699.
8. K. S. Schaffarczyk McHale, R. R. Hawker and J. B. Harper, *New J. Chem.*, 2016, **40**, 7437-7444.
9. R. R. Hawker, R. S. Haines and J. B. Harper, *Chem. Commun.*, 2018, **54**, 2296-2299.